Report 2012

AD-630747

DAVID TAYLOR MODEL BASIN
WASHINGTON, D.C.

DEPARTMENT OF THE NAVY

HYDROMECHANICS

O

AERODYNAMICS

O

STRUCTURAL MECHANICS

O

APPLIED MATHEMATICS

O

ACOUSTICS AND VIBRATION

TESTS OF MACHINED MULTILAYER SPHERICAL SHELLS WITH CLAMPED BOUNDARIES UNDER EXTERNAL HYDROSTATIC PRESSURE

by

Kanehiro Nishida

Distribution of This Document is Unlimited

STRUCTURAL MECHANICS LABORATORY
RESEARCH AND DEVELOPMENT REPORT

August 1965

Report 2012

TESTS OF MACHINED MULTILAYER SPHERICAL SHELLS WITH CLAMPED BOUNDARIES UNDER EXTERNAL HYDROSTATIC PRESSURE

by

Kanehiro Nishida

August 1965

Report 2012
S-R011 01 01
Task 0401

TABLE OF CONTENTS

LIST OF FIGURES

LIST OF TABLES

ABSTRACT

Six spherical shell models with clamped boundaries consisting of two and four layers were tested under external hydrostatic pressure to explore the feasibility of multilayer construction for application to hydrospace vehicles. In addition, four monolithic models were tested to provide a basis of comparison. Three of the multilayer shells were bonded with epoxy resin and the remaining three were not bonded. The bonded multilayer shell models collapsed at pressures approximately equal to that of the monolithic shells. The unbonded shells showed appreciable reduction in strength.

ADMINISTRATIVE INFORMATION

The work described in this report was conducted as part of the Model Basin Fundamental Research Program, Subproject S-R011 01 01, Task 0401.

INTRODUCTION

One of the problems involved in designing pressure hulls for deep-diving oceanographic vehicles and submarines is the increased thickness of the hull plating. As pressure hulls are designed for greater depth and/or larger diameters, the thicknesses required become prohibitive from a fabrication standpoint. Several possible solutions to this problem are being investigated. Among these are the use of sandwich and multilayer construction.

The use of laminated or multilayer construction is quite common in the fabrication of pressure vessels subjected to internal hydrostatic pressure. The use of thinner plating offers the advantage of greater ease in fabrication. Inherently, the thinner plating will be superior in ductility and toughness, higher in yield strength and more uniform in properties. In addition, internal pressure vessels of laminated construction may be made more efficient structurally through prestressing.

However, the use of multilayer construction for pressure hulls of hydrospace vehicles introduces a problem which is not encountered in internal pressure applications, namely that of structural stability. Little effort has been directed towards the evaluation of this problem.

Six multilayer and four monolithic spherical caps were machined and tested under external pressure to explore the feasibility of multilayer spherical shells for hydrospace applications. The six multilayer spherical caps consisted of two and four layers. Three of these models were bonded with epoxy resin and the remaining three were not bonded. The four monolithic shells were tested to provide a direct basis of comparison. The spherical cap with clamped boundaries was chosen as the model configuration because it was felt that the presence of high bending stresses would be a severe test of the efficiency of multilayered spherical shells. This report presents the results of these tests.

DESCRIPTION OF MODELS

Ten models, each consisting of a spherical cap bounded by a heavy end cylinder, were machined from 7075-T6 aluminum bar stock with a nominal yield strength of 80,000 psi. Young's modulus E and Poisson's ratio ν were assumed to be 10.8 x 10^6 psi and 0.3, respectively, in all calculations. A schematic section view of the models is presented in Figure 1. Figure 2 is a plot of the ratio of $(E_s E_t)^{\frac{1}{2}}$ to E and the axial compressive stress in the material as determined from uniaxial compression test of specimens taken from the bar stock, where E_s and E_t are the secant and tangent moduli respectively.

The ten models comprised two groups of shells, one with a nominal shell thickness of 0.03 in. and the other 0.06 in. The 0.03 group consisted of monolithic and two-layer models, and the 0.06 group consisted of four-layer models in addition to monolithic and two-layer models. Each model had an included angle of 90 deg. Earlier tests have indicated that the strength of segments of these thicknesses is not affected by increasing the size of the segment beyond 90 deg; see Appendix A.

Table 1 gives the nominal model dimensions, and Table 2 presents the shell thicknesses and measured initial departures from sphericity. The thicknesses shown for the multilayered shells were obtained by adding the thicknesses of the individual layers in corresponding areas. Radius measurements for these models were taken on the inside surfaces of the assembled models with the edges clamped. For the bonded models, these measurements were taken prior to bonding.

All models or layers were machined in the same manner. First both surfaces were rough machined. Then the inside contour was generated with a special tool while the outside was supported with a potlike fixture formed of the low melting point material serol. The final outside contour was then obtained by supporting the inside contour with a mandrel and generating the outside surface.

Models 6, 8, and 9 were bonded with epoxy resin (Epon 828 and Versimid 140) having a compressive yield strength of about 7000 psi and a Young's modulus of 330,000 psi. The entire mating surfaces were coated, the layers were slipped together, and then firmly clamped at the edges. Application of heat was necessary to solidify the epoxy resin. This was done in a furnace at a temperature of 140 F for 1 hr. Models 5, 7, and 10 were not bonded.

TEST PROCEDURE

Each model was tested under external hydrostatic loading with oil as the pressure media. A sketch of a model in the test tank is presented in Figure 3. Pressure was applied in increments, and effort was made to minimize pressure surge when applying the load. Each increment of pressure was held at least 1 min and the final pressure increment was less than 5 percent of the collapse pressure. A slight dropoff in pressure was observed just prior to collapse of all models. As soon as this was detected, the pressure was increased to maintain a constant level.

Strain readings were recorded for each model except Models 2, 4, and 6. Because of the relatively small size of the models, foil resistance strain gages with grids 1/32 x 1/32 in. were used. Strain gage locations for these models are given in Figure 5.

RESULTS

The experimental and calculated collapse pressures and membrane stresses away from the boundary are presented in Table 3. Elastic strain data for all instrumented models are presented in Figure 4. The abscissa for these plots is the ratio of the arc length from the fixed edge to the gage to one-half the unsupported arc length of the shell, and the ordinate is the strain sensitivity (i.e., the initial slope of the straight-line portion of the pressure strain curve in μ in./in./psi). Typical pressure strain diagrams are presented on Figure 5. Photographs of the models after tests are shown in Figure 6.

DISCUSSION

Table 3 compares the experimental buckling pressures with the pressures calculated by Model Basin empirical elastic and inelastic buckling equations* for complete spheres. In all calculated pressures, the average thickness near the edge was used since failure of each of these models occurred in the nonsymmetric mode (see Figure 6).

The experimental buckling pressures of the monolithic models are in good agreement with previous results of Krenzke and Kiernan.[1] Models 1 and 2, which had a P_3/P_E ratio of approximately 1 and a θ value of 11.8, gave P_{EXP}/P_E ratios of 0.76 and 0.78, respectively. For the same values of P_3/P_E and θ, a P_{EXP}/P_E ratio of approximately 0.80 has been obtained in the earlier tests.[1] Models 3 and 4 which had a P_3/P_E ratio of approximately 1.7 and a θ value of 8.2 gave P_{EXP}/P_E ratios of 0.80 and 0.81, respectively. For the same values of P_3/P_E and θ, a P_{EXP}/P_E ratio of approximately 0.86 had been obtained in the earlier tests.[1]

The experimental results of the bonded multilayer shells were essentially the same as those of the monolithic models (see Table 3). The bonded model of the 0.03 in.

[1] References are listed on page 38

*A brief background on the collapse strength of spherical shells together with the nomenclature used in this text are presented in Appendix A.

series (Model 8) showed no reduction in strength. In fact, the ratio of P_{EXP}/P_E for Model 8 was slightly higher than that obtained for the monolithic shells. This is possibly attributable to the thickness of the epoxy resin layer which is neglected in all calculations. Models 6 and 9, the bonded models of the 0.06-in. series, showed a reduction in strength of approximately 9 percent. P_{EXP}/P_E ratios of 0.75 and 0.74 were obtained for these models. Models 3 and 4, which were monolithic in construction and had the same ratio of shell thickness to radius, gave P_{EXP}/P_E ratios of 0.80 and 0.81. Conceivably, failure of these models could have initiated prematurely in the bonding layer.

The collapse strength of the unbonded models was appreciably less than that of the monolithic models of comparable shell thickness. Models 5, 7 and 10 collapsed at pressures equal to 77, 73, and 48 percent of those observed for comparable monolithic shells. Considering the severe edge conditions imposed on these shells, these results are not too surprising. In explaining the strength reduction of these shells, it is convenient to put Zoelly's classical buckling equation[2] in the form

$$P_1 = \frac{4\sqrt{(1-\nu^2)BD}}{R^2} \qquad [1]$$

where B, the extensional stiffness, is equal to $Eh/1 - \nu^2$ and D, the bending stiffness, is equal to $Eh^3/12(1-\nu^2)$. In this equation, it can be seen that the only term affected by layered construction is the bending stiffness D. Assuming the layers are free to slip on one another, the effective stiffness becomes

$$D_{EFF} = \frac{(j)\ E\ (h/j)^3}{12(1-\nu^2)} = \frac{1}{j^2}\ D \qquad [2]$$

where j is the number of equal thicknesses comprising the shell. If this expression is used in place of the nominal bending stiffness D in Equation [1], the buckling expression becomes

$$P_{1EFF} = \frac{4}{j} \frac{\sqrt{(1 - \nu^2)BD}}{R^2} \qquad [3]$$

Thus, it seems that an initially perfect, multilayer sphere could be weaker in strength by a factor of 1/j when compared to a monolithic shell of the same thickness and radius. If the factor 1/j is used in conjunction with Model Basin empirical equations, the elastic and inelastic buckling of near-perfect multilayer shells becomes

$$P_{3EFF} = 1/j \quad (.84)E \ (h/R_o)^2 \quad \text{for} \quad \nu = 0.3 \qquad [4]$$

$$P_{E_{EFF}} = 1/j \quad (.84) \sqrt{E_s E_t} \ (h/R_o)^2 \quad \text{for} \quad \nu = 0.3 \qquad [5]$$

The experimental results of Models 5, 7, and 10 are compared with the pressures of Equations [4] and [5] in Table 3. It can be seen that fairly good agreement was obtained on Models 7 and 10, both of which seemed to have failed elastically. $P_{EXP}/P_{E_{EFF}}$ ratios of 1.10 and 0.94 were obtained for these models. The fairly low nominal stress levels attained at collapse (59 and 45 percent of the stress at the proportional limit) indicates that these models failed essentially by elastic instability. Although some nonlinearity can be observed in the pressure strain plots of both these models, this is attributed to elastic nonlinear behavior. This is indicated in the pressure strain plots for Model 7 (Figure 5) where the shape of the curves was repeated without noticeable permanent set between the two runs.

A $P_{EXP}/P_{E_{EFF}}$ ratio of 0.74 was obtained on Model 5. Although the nominal stress at collapse was only 74 percent of the proportional limit, the pressure strain plot for this model (Figure 5) indicates that yielding occurred prior to failure. Thus, failure of Model 5 was inelastic. It is therefore not surprising to see the fairly low ratio of $P_{EXP}/P_{E_{EFF}}$. Similar results have been obtained for comparable monolithic segments; see Figure 7.

Figures 4a and 4b indicate that there was relatively good agreement between experimental and theoretical strains for the monolithic shells (Models 1 and 3).* The general shape of the strain distribution patterns was very similar, but the experimental points were slightly to the left of the theoretical curve. The experimental results of the bonded multilayer shells (Model 3 and Models 6 and 9) are also shown on these plots. Note that the strains were nearly identical to those of the monolithic shells. The strains for Model 4 and Models 5 and 10 which were not bonded are compared to the empirical distribution of experimental strains of Models 1 and 3 in Figures 4c and 4d. The data indicate that the edge effects on the unbonded models were confined closer to the boundary than on the monolithic shells. This is attributed to the reduced stiffness of the multilayer shell. The data also demonstrate that, as would be expected, considerably more bending was present in the unbonded shells than in the bonded and monolithic shells. This supports the conclusion that premature failure results from the reduced bending rigidity of unstable multilayer spherical segments which are not bonded together.

*The elastic stress analysis of spherical segments with clamped boundaries is presented in Appendix B.

Although these tests were rather exploratory, several general observations can be made concerning the feasibility of laminated shells for deep-depth applications. The models tested in this study were in the farily unstable range with severe edge conditions, and thus the results should be used with caution. It is possible that the strength of a laminated shell without bonding can be increased by providing more favorable edge conditions. The collapse strength of a complete multilayer sphere, for example, could approach that of a monolithic sphere if no appreciable bending is present prior to collapse. In this regard, the effect of bending, friction between layers, and reduced bending rigidity on collapse strength must be more firmly established. If the individual layer of a multilayer shell is of such thickness that it is fairly stable in itself, these effects are not too significant. This is true for many of the materials under consideration for various hydrospace applications. Thus, further investigation of this problem seems warranted.

SUMMARY

Six multilayer and four monolithic spherical segments with clamped edges were tested under hydrostatic pressure to explore the feasibility of laminated spherical shells for hydrospace applications. These tests demonstrated that the bonded multilayer shells were approximately equal in strength to the monolithic shells. However, the collapse strength of those multilayer shells which were not bonded was appreciably below that of the monolithic shells. In fact, the strength of the unbonded shells which failed at low membrane stress levels could be estimated by neglecting the effects of frictional forces between the layers. Since the models tested were fairly unstable and had severe edge conditions and since many practical applications might involve stable spheres or hemispheres with more ideal edge conditions than represented by these models, further investigation of the behavior of multilayer spherical shells appears warranted.

ACKNOWLEDGMENTS

The author is indebted to Messrs. T.J. Kiernan and M.A. Krenzke for their valuable comments during the conduct of the project and the preparation of this report. The theoretical analysis of stresses in spherical segments was accomplished by Mr. F.M. Schwartz.

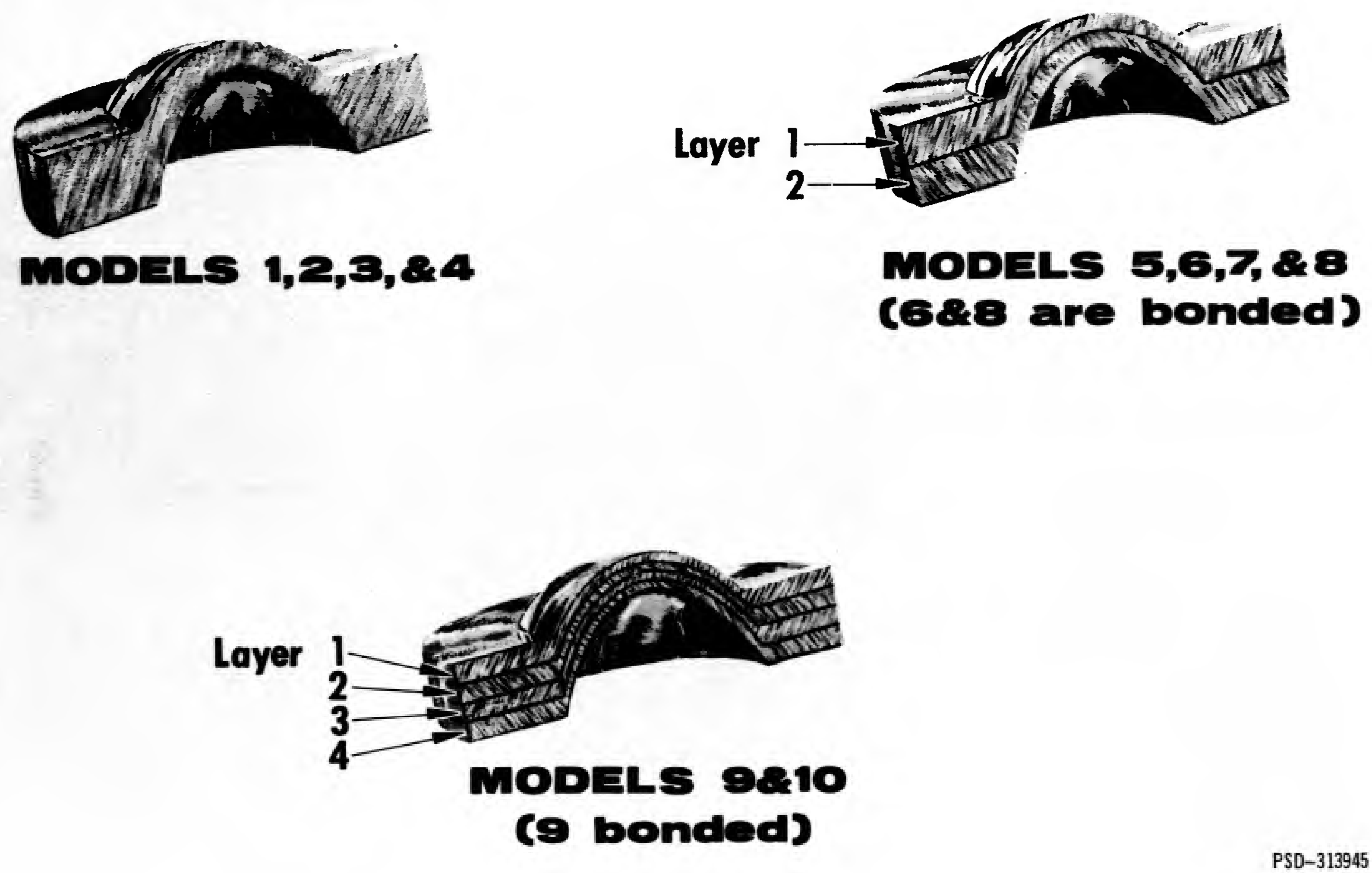

Figure 1 – Schematic Section View of Models

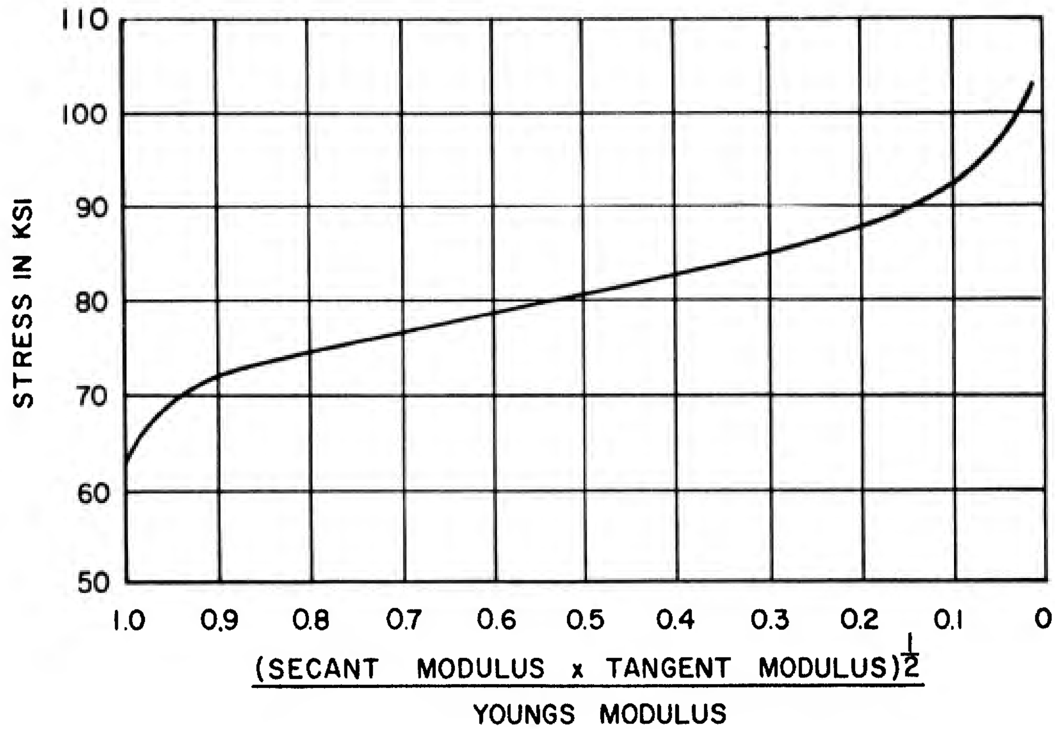

Figure 2 – Representative Material Characteristics

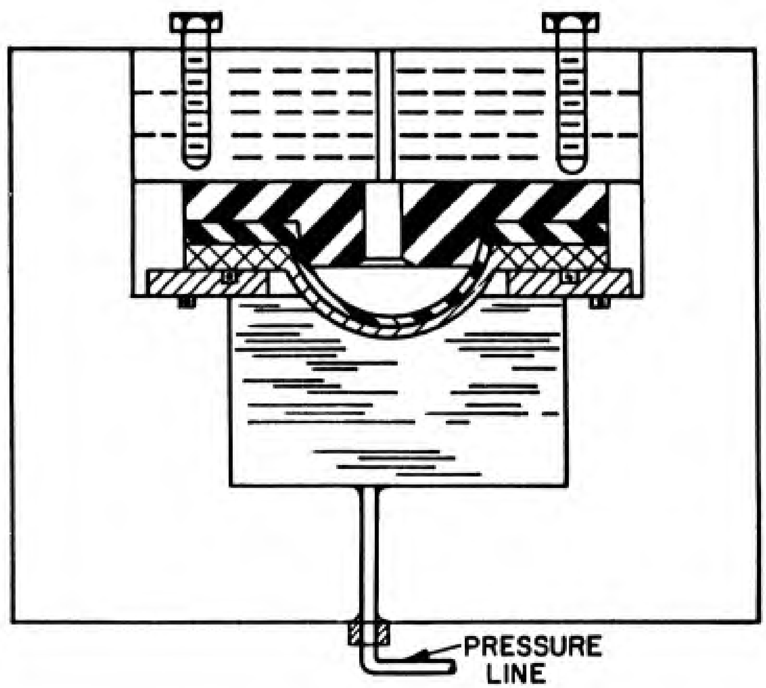

Figure 3 – Sketch of Model in Pressure Tank

Figure 4 – Comparison of Experimental and Theoretical Strains

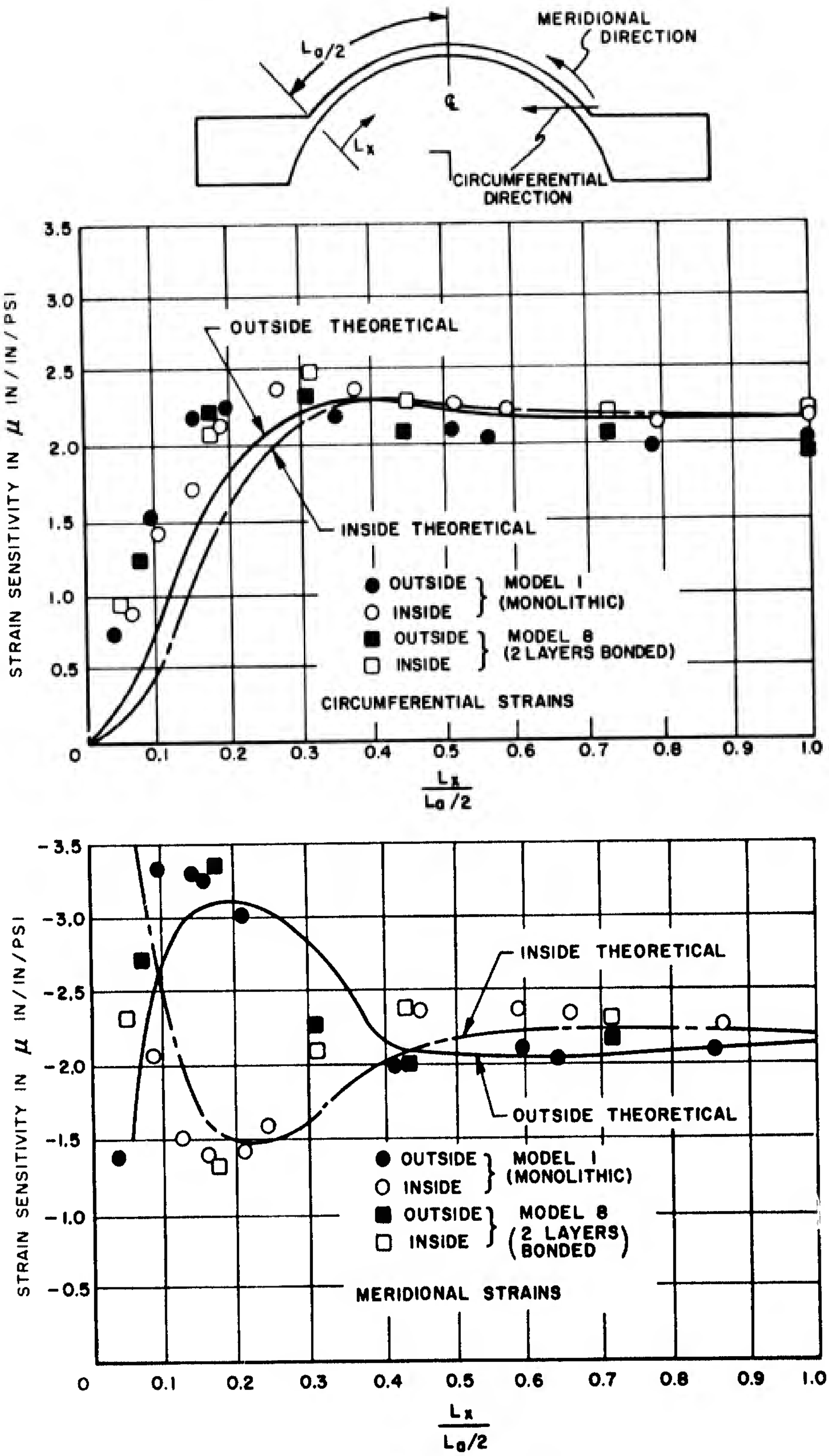

Figure 4a – Models 1 and 8

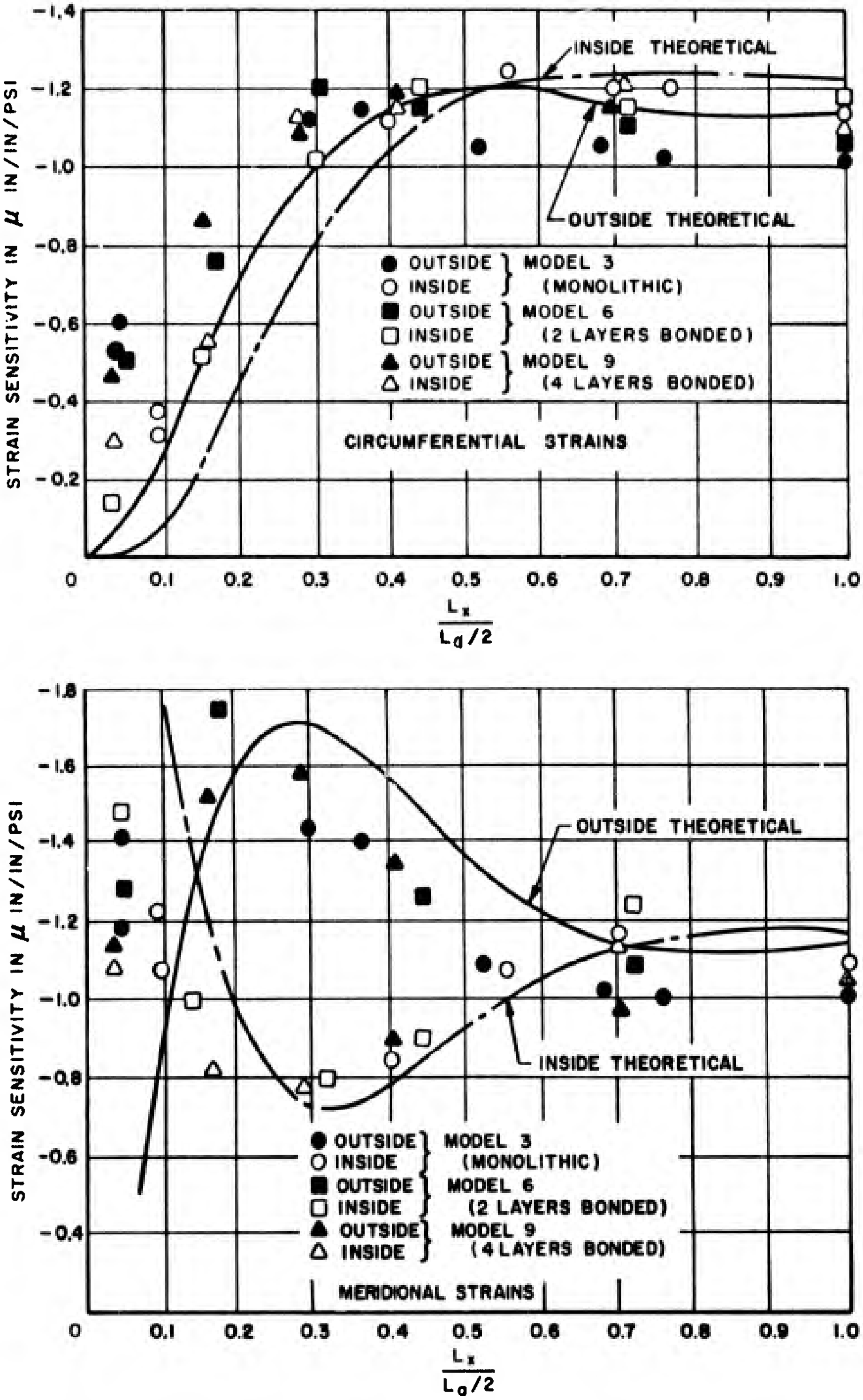

Figure 4b – Models 3, 6, and 9

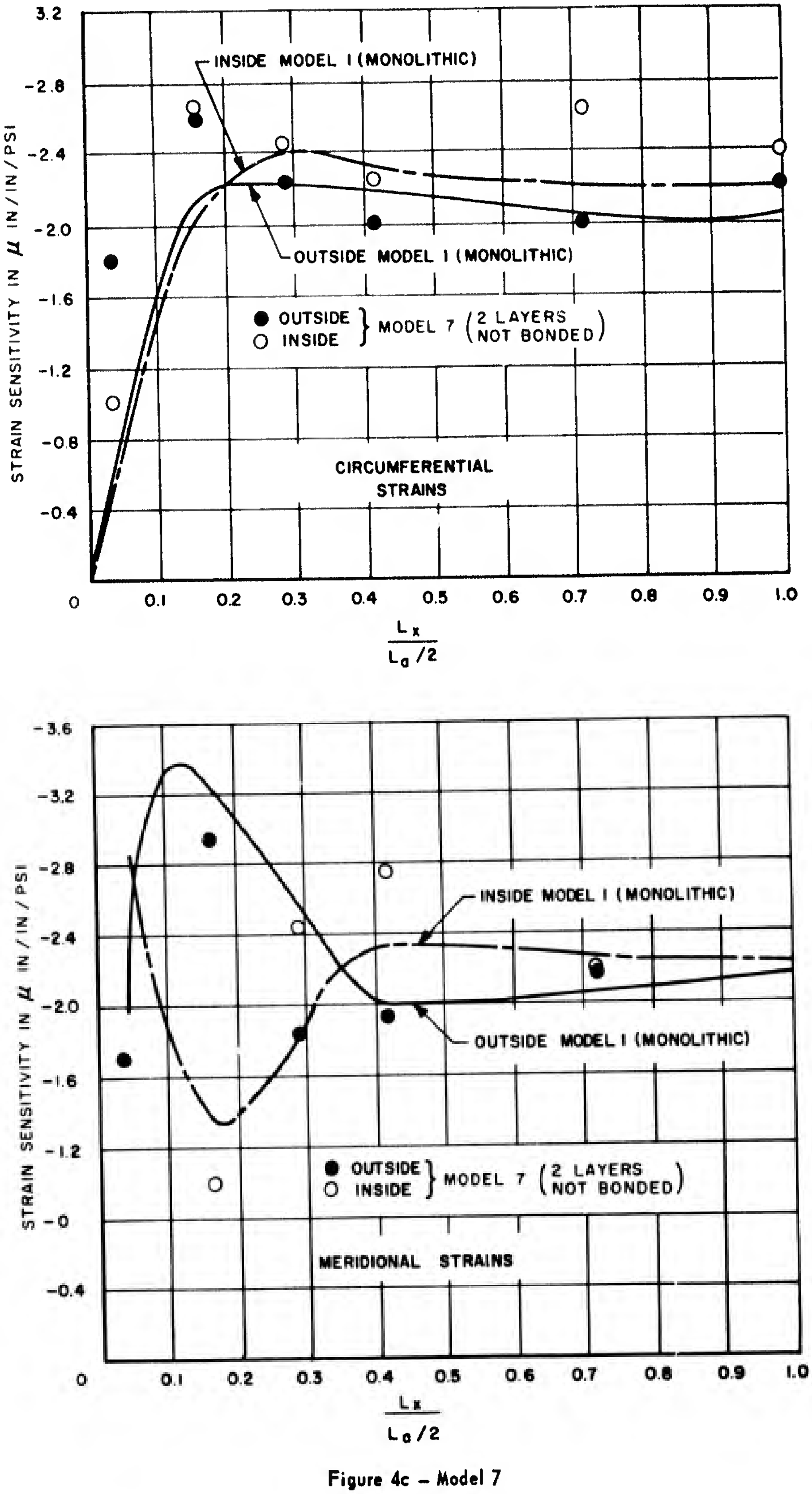

Figure 4c – Model 7

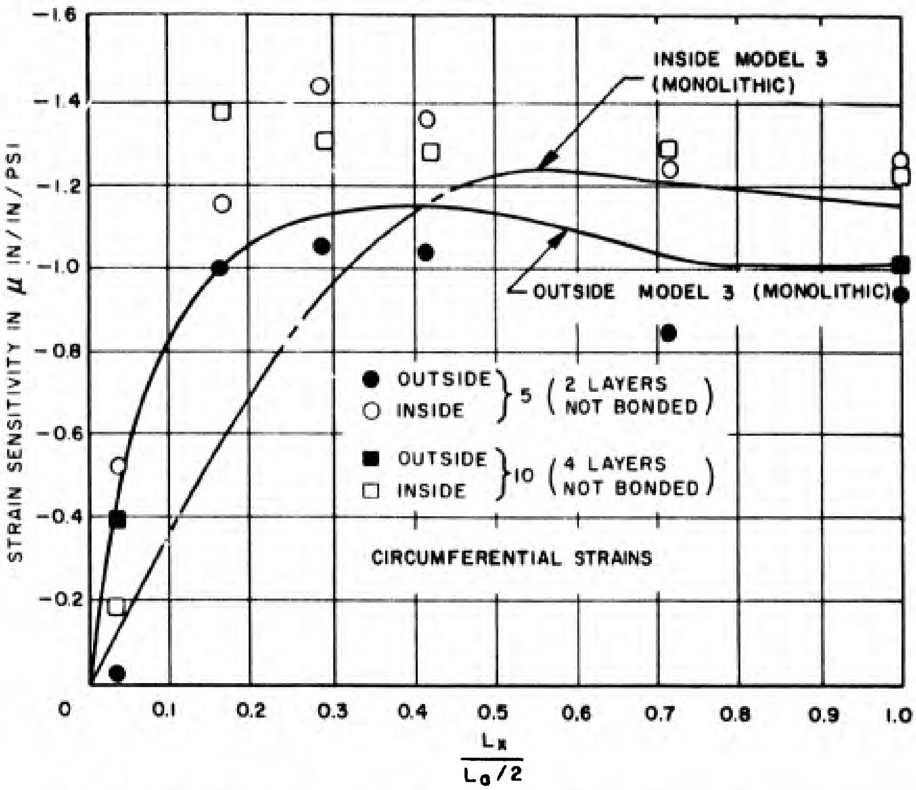

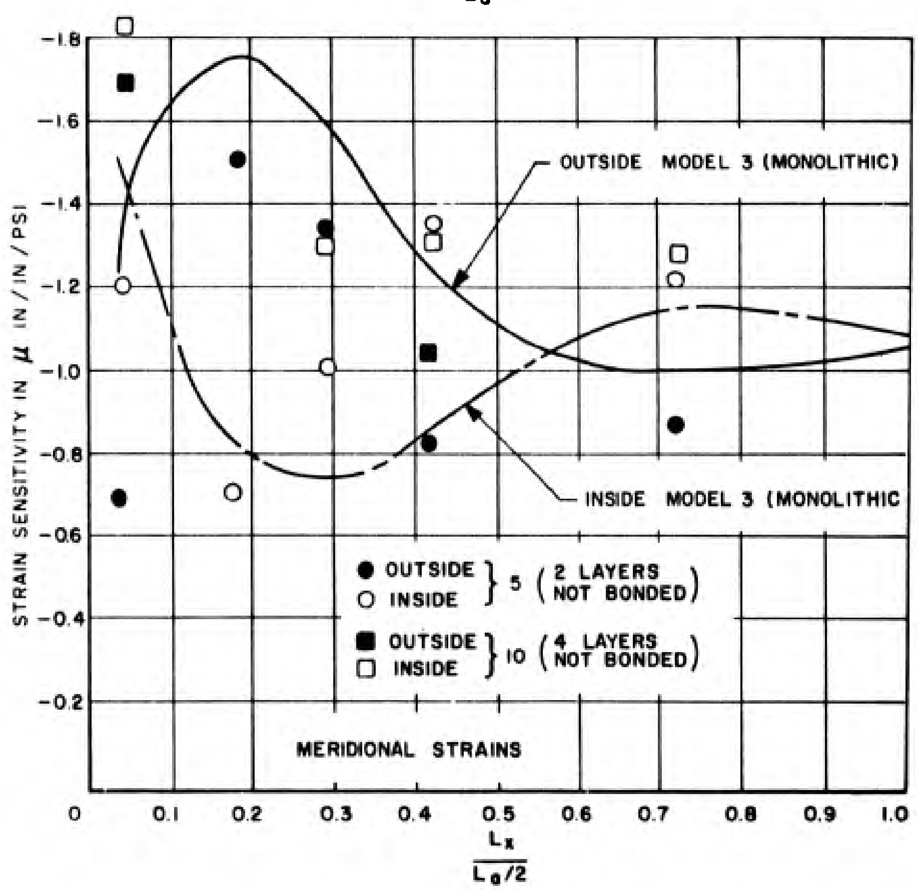

Figure 4d – Models 5 and 10

Figure 5 – Typical Pressure Strain Diagrams

The gage locations are identified at base of each curve. The first letter (I or O) indicates inside or outside location, the second letter (C or M) indicates circumferential or meridional orientation and the numbers are the $L_x / \frac{L_a}{2}$ ratio. The strain sensitivities are given in parenthesis.

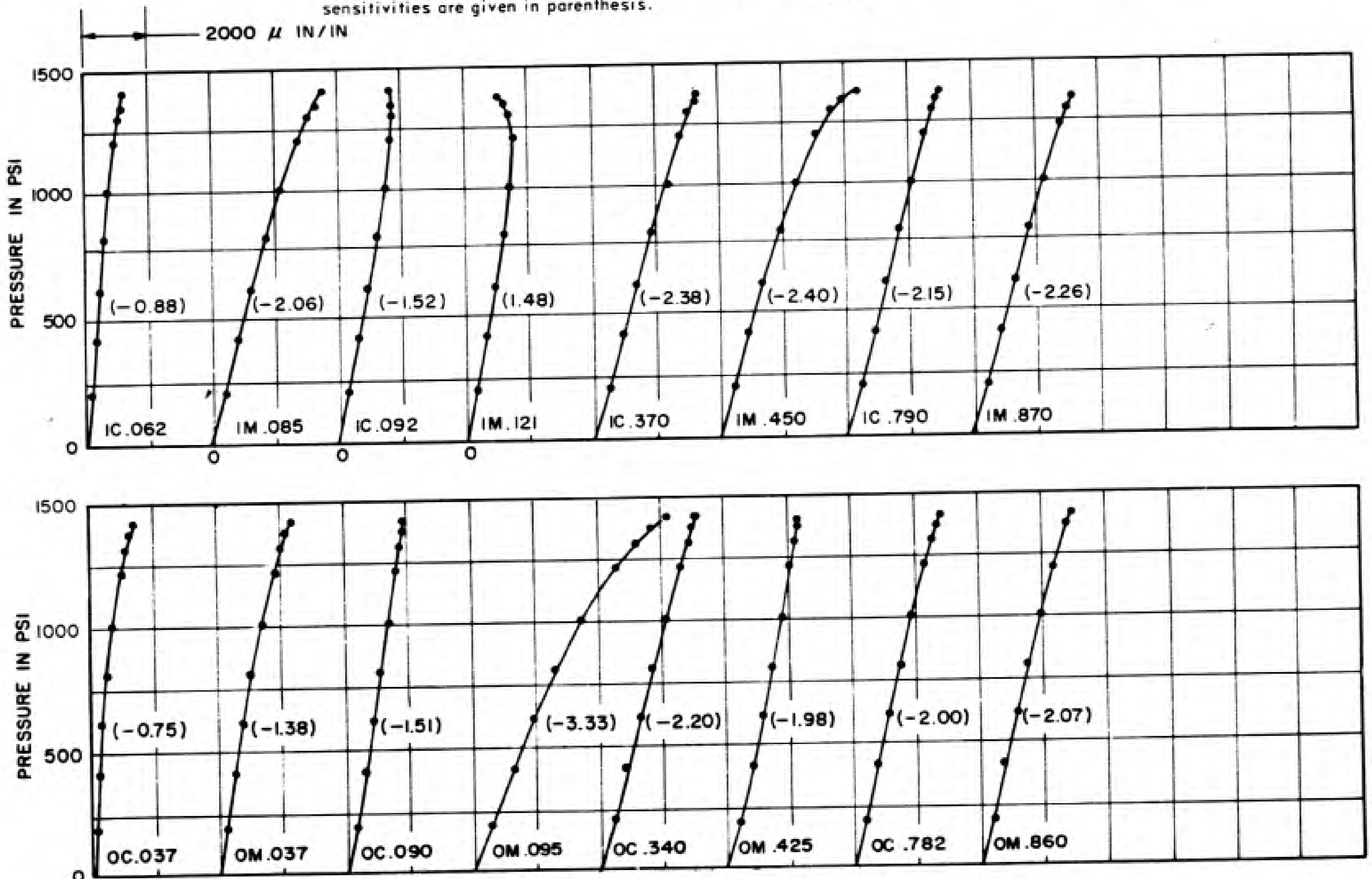

Figure 5a – Model 1

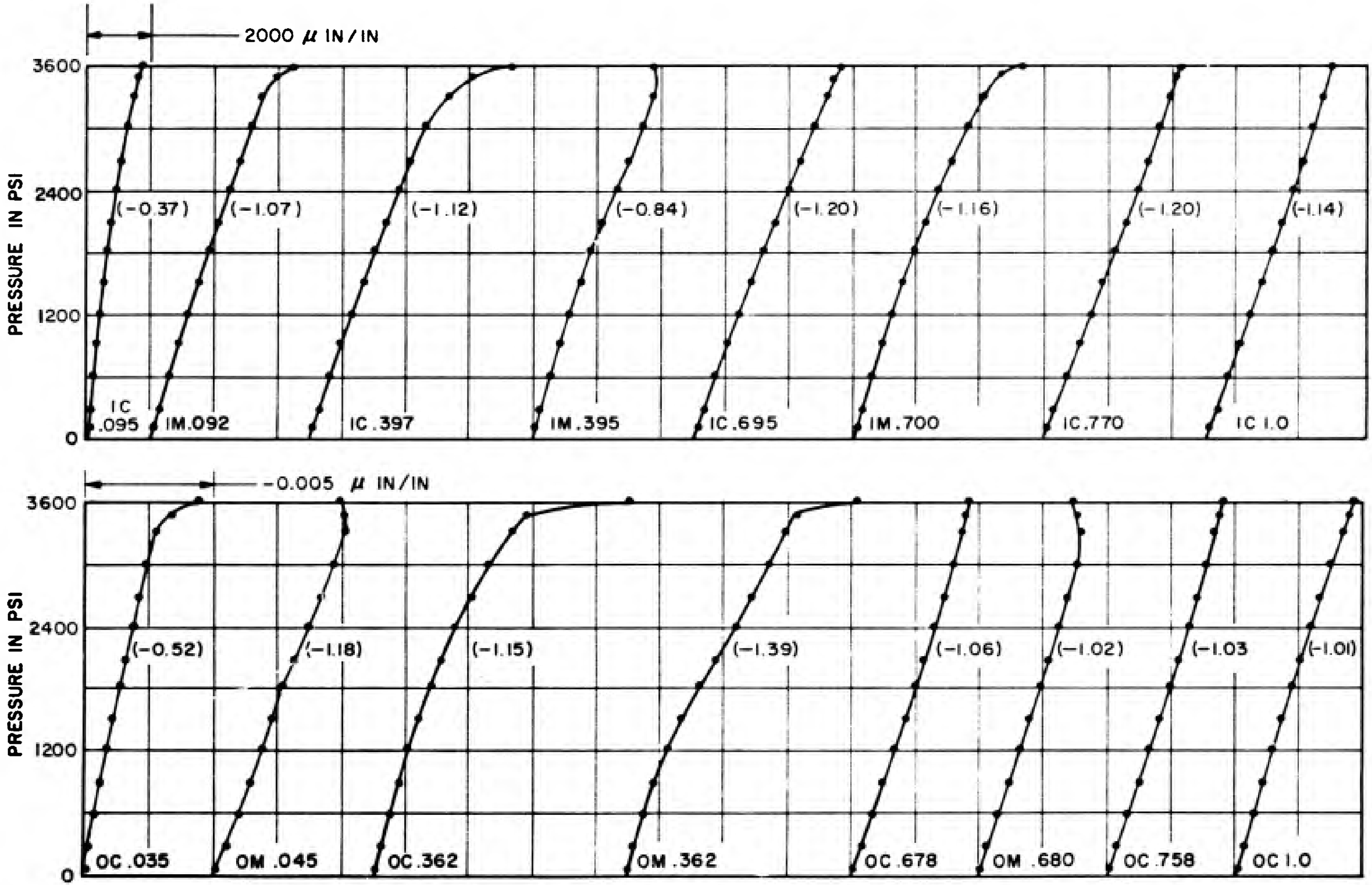

Figure 5b – Model 3

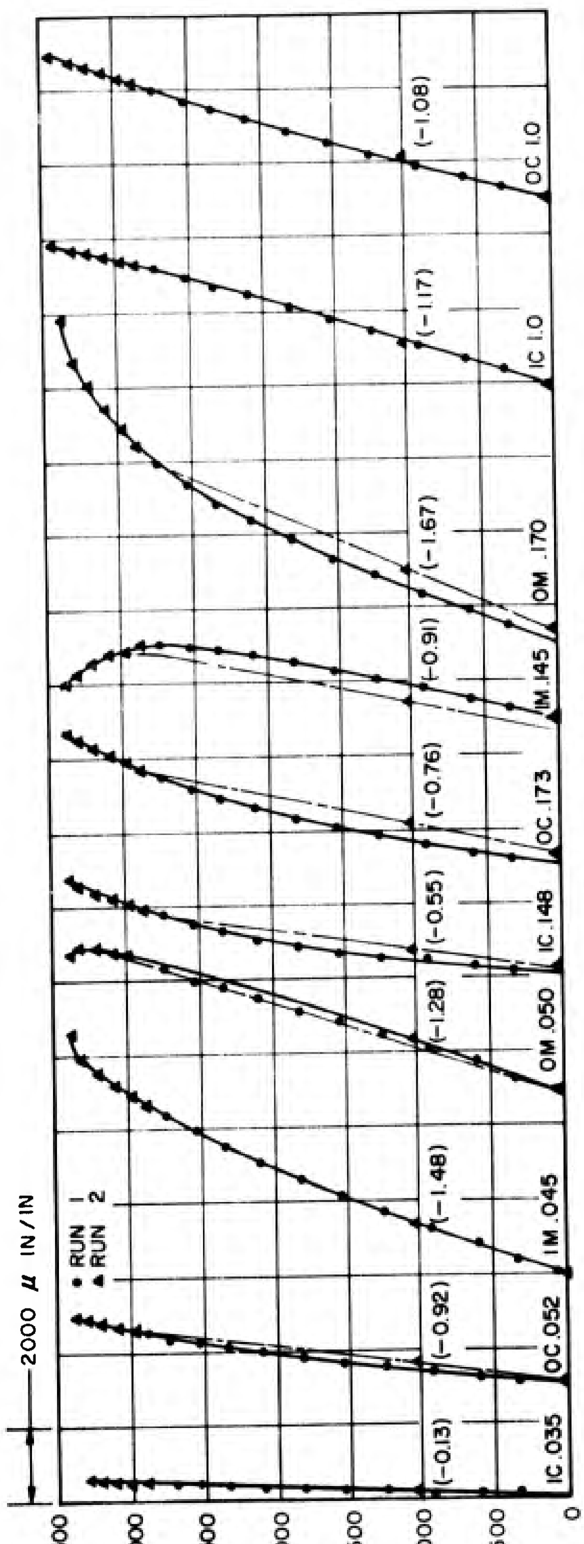

Figure 5c - Model 6

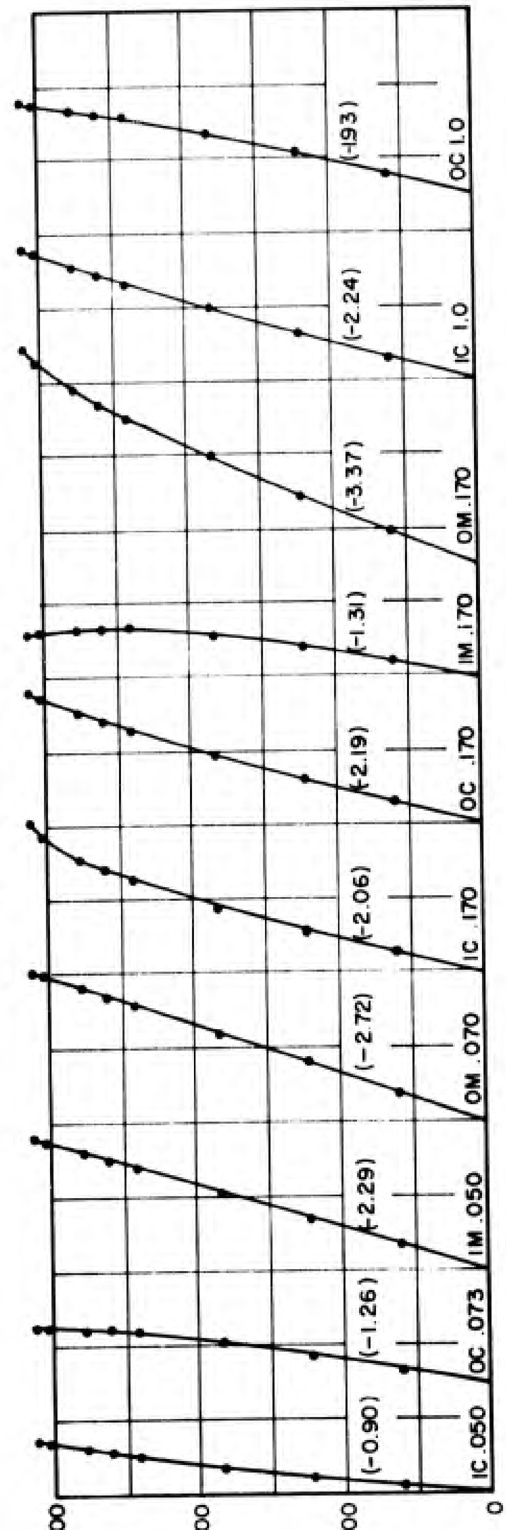

Figure 5d - Model 8

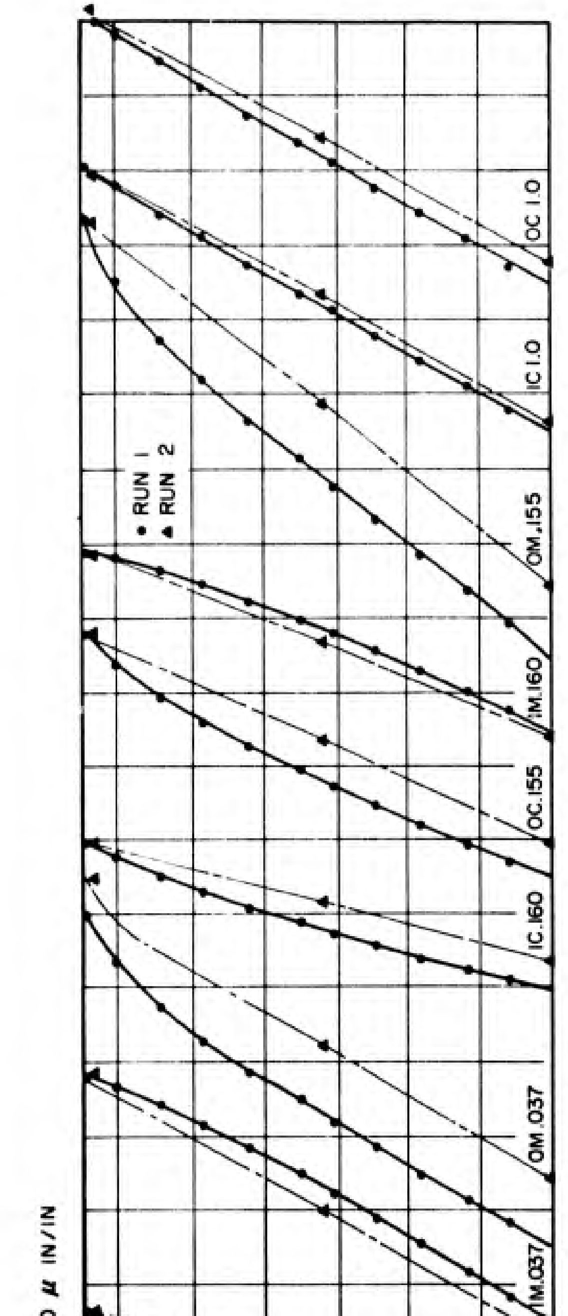

Figure 5e – Model 9

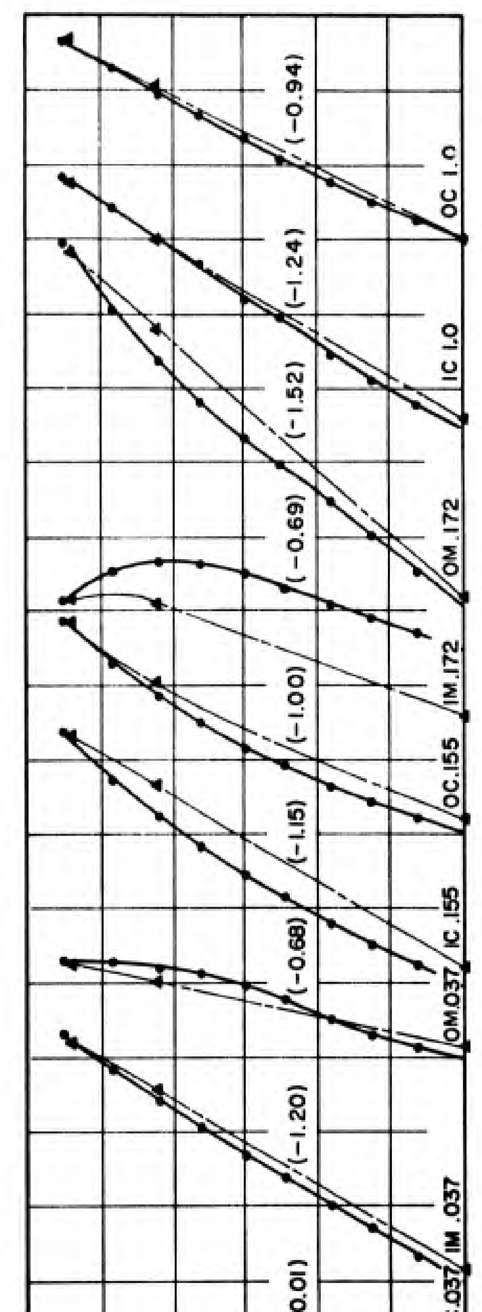

Figure 5f – Model 5

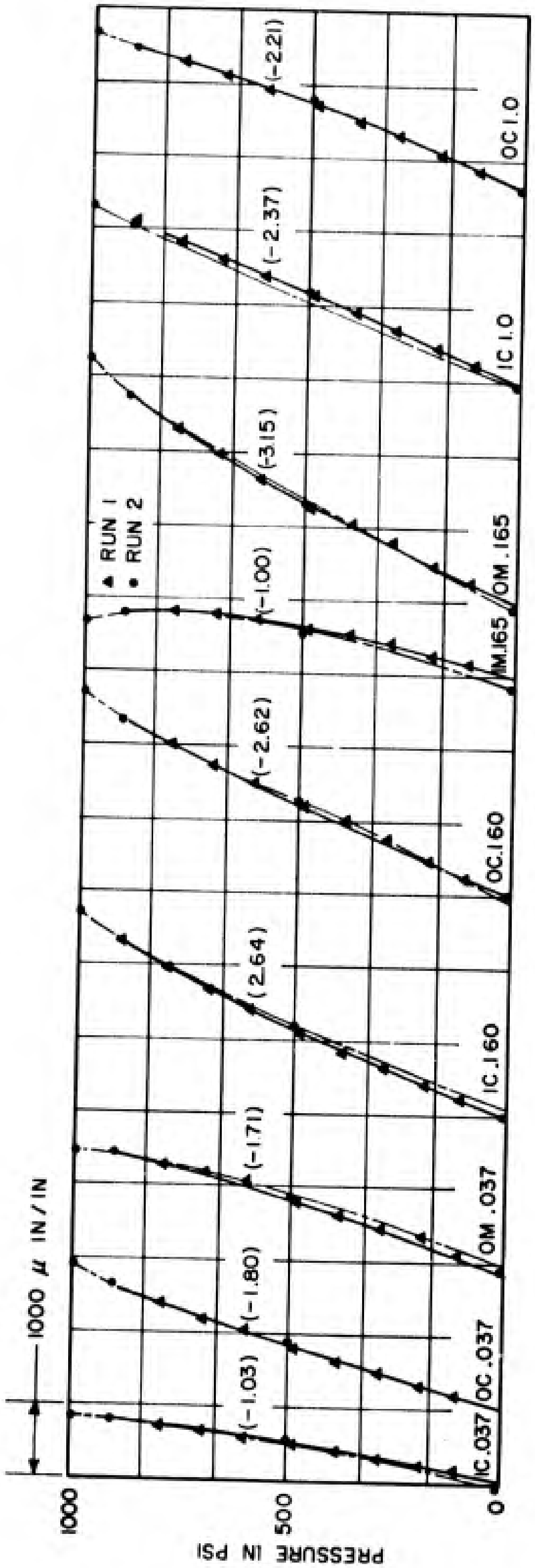

Figure 5g – Model 7

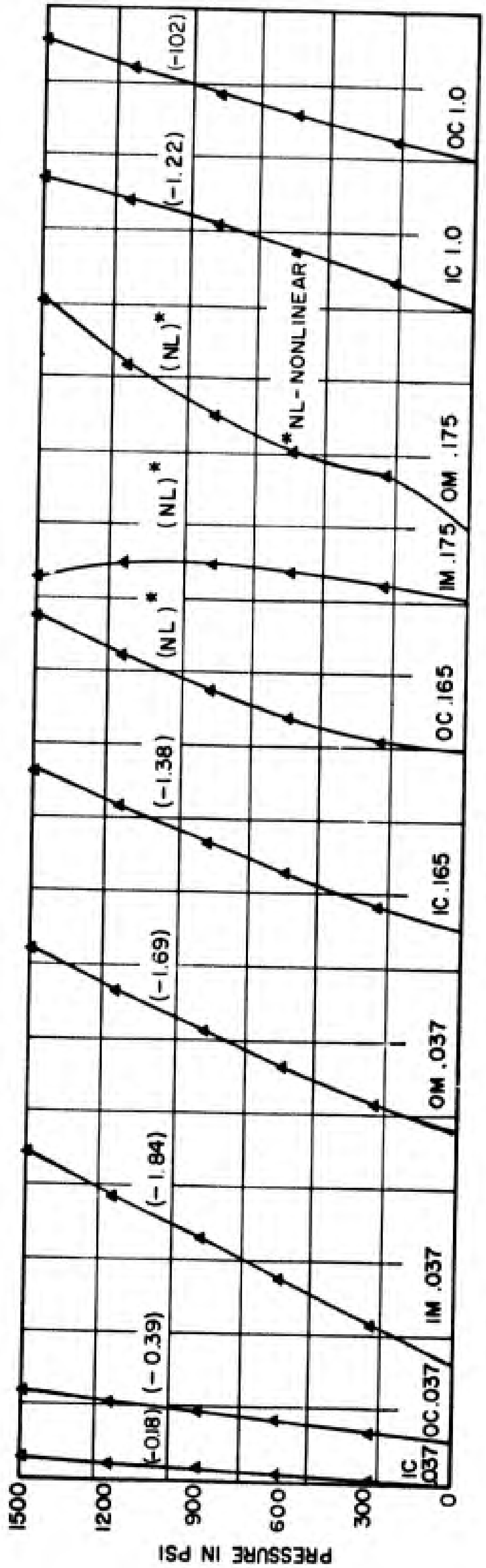

Figure 5h – Model 10

Figure 6 – Models after Collapse

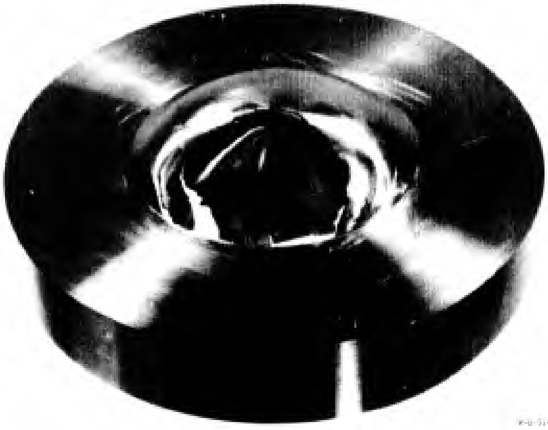

Model 1

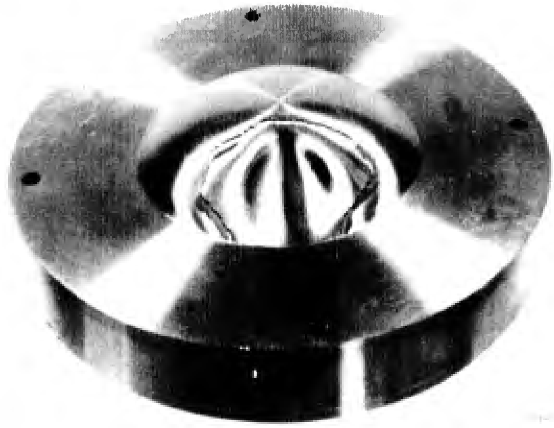

Model 2

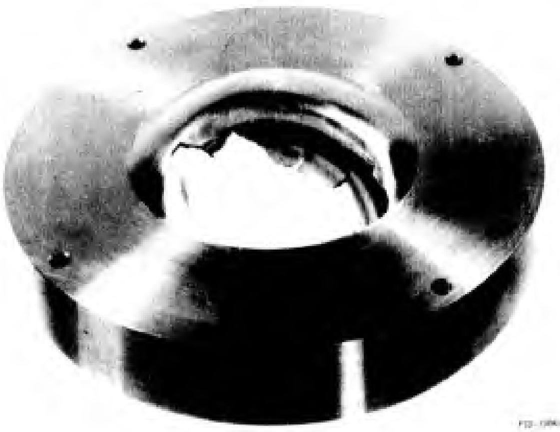

Model 3

Model 4

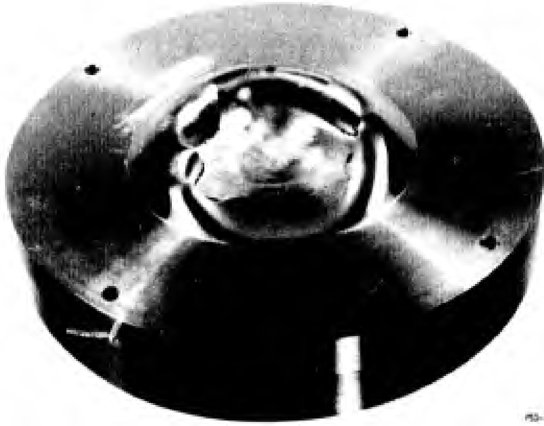

Model 5

Figure 6 (Continued)

Model 6

Model 7

Model 8

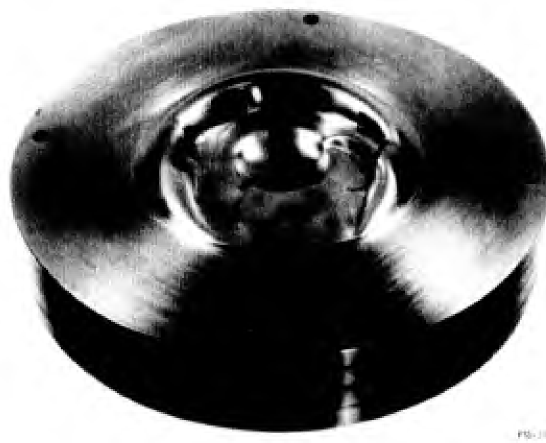

Model 9

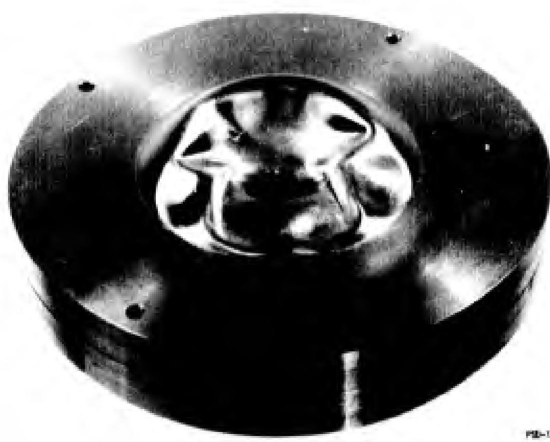

Model 10

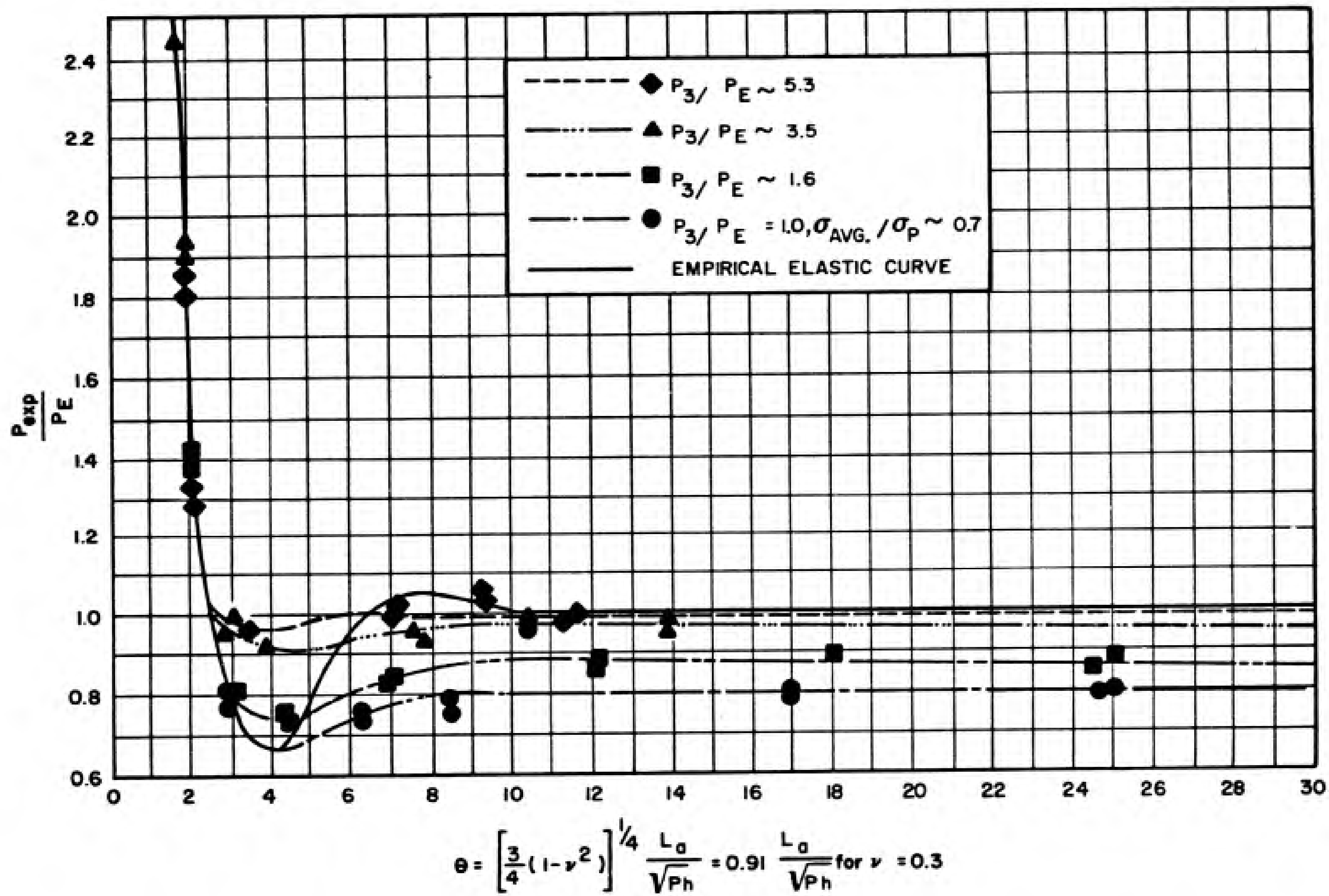

Figure 7 – Experimental Inelastic Buckling Data for Spherical Shells with Clamped Edges

TABLE 1
Nominal Model Dimensions

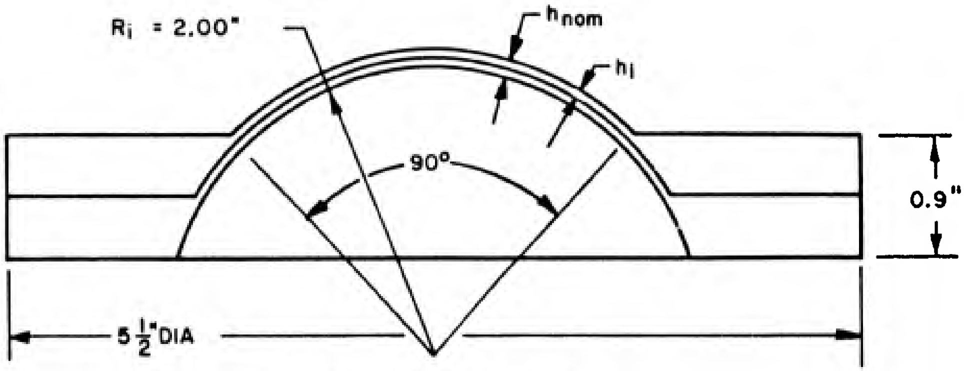

TYPICAL CROSS SECTION

Model Number	Number of Layers	h_{nom}	h_i
1	1	0.03	0.03
2	1	0.03	0.03
3	1	0.06	0.06
4	1	0.06	0.06
5	2	0.06	0.03
6	2*	0.06	0.03
7	2	0.03	0.015
8	2*	0.03	0.015
9	4*	0.06	0.015
10	4	0.06	0.015

*Bonded

TABLE 2

Measured Spherical Wall Thickness and Initial Departures from Sphericity

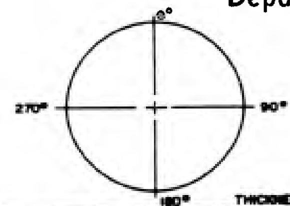

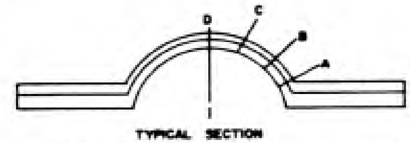

THICKNESS MEASUREMENTS**

DEPARTURES FROM AVERAGE MEASURED INSIDE RADIUS

Model Number	Number of Layers	Horizontal Orientation Deg	Vertical Orientation A	B	C	D	Average Measured Inside Radius Inches	Vertical Orientation A	B	C	D
1	1	0	0.0295	0.0297	0.0296	0.0297	2.0009	-0.0001	-0.0001	0	0
		90	0.0295	0.0297	0.0296						
		180	0.0295	0.0297	0.0296						
		270	0.0295	0.0297	0.0296						
2	1	0	0.0296	0.0298	0.0296	0.0291	1.9999	0	-0.0001	-0.0001	+0.0005
		90	0.0296	0.0298	0.0296						
		180	0.0296	0.0298	0.0296						
		270	0.0296	0.0298	0.0296						
3	1	0	0.0595	0.0596	0.0597	0.0595	2.0010	0	0	0	-0.0001
		90	0.0595	0.0596	0.0597						
		180	0.0595	0.0596	0.0597						
		270	0.0595	0.0596	0.0597						
4	1	0	0.0597	0.0597	0.0597	0.0596	2.0010	-0.0001	0	0	-0.0001
		90	0.0597	0.0597	0.0597						
		180	0.0597	0.0597	0.0597						
		270	0.0597	0.0597	0.0597						
5	2	0	0.0600	0.0600	0.0602	0.0593	2.0012	-0.0002	-0.0001	+0.0002	-0.003
		90	0.0599	0.0600	0.0603						
		180	0.0599	0.0600	0.0604						
		270	0.0599	0.0601	0.0601						
6	2*	0	0.0600	0.0598	0.0599	0.0593	2.0004	0	0	-0.0001	-0.0001
		90	0.0599	0.0598	0.0598						
		180	0.0600	0.0598	0.0599						
		270	0.0600	0.0598	0.0598						
7	2	0	0.0294	0.0292	0.0295	0.0292	2.0003	+0.0001	+0.0002	-0.0005	+0.0001
		90	0.0294	0.0293	0.0295						
		180	0.0293	0.0292	0.0294						
		270	0.0292	0.0292	0.0295						
8	2*	0	0.0297	0.0299	0.0303	0.0295	2.0002	0	0	-0.0001	+0.0002
		90	0.0297	0.0299	0.0300						
		180	0.0298	0.0299	0.0303						
		270	0.0298	0.0299	0.0302						
9	4*	0	0.0587	0.0600	0.0604	0.0588	1.9999	-0.0002	0	+0.0002	0
		90	0.0589	0.0599	0.0606						
		180	0.0588	0.0600	0.0604						
		270	0.0581	0.0600	0.0603						
10	4	0	0.0602	0.0599	0.0598	0.0589	2.0006	0	+0.0002	-0.0002	0
		90	0.0603	0.0601	0.0599						
		180	0.0604	0.0603	0.0599						
		270	0.0604	0.0603	0.0598						

* Indicates Bonded Models ** The Thickness Shown For All Multilayer Shells were obtained by adding the thickness of the individual layers

TABLE 3

Summary of Experimental and Calculated Collapse Pressures and Stresses

Nominal Shell Thickness in Inches	Model No.	No. of Layers	P_{EXP}	$\frac{\sigma_{AVG} \text{ at Collapse}}{\sigma \text{ Propor. Limit}}$	P_3**	P_E***	P_3/P_E	P_{EXP}/P_E	$P_{3_{EFF}}$	$P_{E_{EFF}}$	$P_{3_{EFF}}/P_{E_{EFF}}$	$P_{EXP}/P_{E_{EXP}}$
.03	1	1	1440	0.77	1928	1900	1.01	0.76	--	--	--	--
	2	1	1500	0.80	1942	1910	1.01	0.78	--	--	--	--
	8	2*	1595	0.78	1981	1981	1.00	0.80	--	--	--	--
	7	2	1050	0.59	1891	1891	1.00	0.56	950	950	1.00 (elastic)	1.10
.06	3	1	3600	1.05	7589	4500	1.69	0.80	--	--	--	--
	4	1	3640	1.06	7615	4510	1.69	0.81	--	--	--	--
	6	2*	3400	0.95	7669	4530	1.70	0.75	--	--	--	--
	9	4*	3270	0.89	7622	4400	1.73	0.74	--	--	--	--
	5	2	2775	0.74	7712	4450	1.73	0.62	3860	3750	1.03	0.74
	10	4	1795	0.45	7665	4630	1.66	0.39	1920	1920	1.00 (elastic)	0.94

*Bonded
**Model Basin Empirical Elastic Buckling Equation
***Model Basin Empirical Elastic Buckling Equation

APPENDIX A
RECENT TESTS OF SPHERICAL SHELLS

The elastic buckling of complete spherical shells was first treated by Zoelly and is presented by Timoshenko.[2] His classical pressure P_1 may be given by

$$P_1 = 1.21\ E\ (h/R)^2 \quad \text{for } \nu = 0.3 \qquad [A\ 1]$$

where h is the shell thickness and R is the midsurface radius of the shell.

Early experiments showed wide disagreement with Equation [A 1]. Normally, this disagreement may be attributed to initial imperfections, adverse boundary conditions, and residual stresses present in the experimental specimens. More recent tests[1,3,4] of shells which more closely meet the assumption of the theory (i.e., near-perfect shells) lend considerable support to Zoelly's equation. Tests of small, near-perfect machined hemispherical shells which had ideal boundaries and which failed at stress levels below the proportional limit have given experimental pressures ranging from 70 to 90 percent of the classical buckling pressure. The tests indicated that the classical buckling coefficient of 1.21 may be attainable for the ideal spherical shell. However, the tests also demonstrate that for small, almost unmeasurable imperfections, the buckling coefficient falls off very rapidly to about 70 percent of the classical value. Based on these results, the Model Basin recommended[1,3,4] that the following formula be used to predict the collapse strength of near-perfect spherical shells whose initial departures from sphericity are less than 2 1/2 percent of the shell thickness:

$$P_3 = 0.84\ E\ (h/R_o)^2 \quad \text{for } \nu = 0.3 \qquad [A\ 2]$$

where R_o is the radius to the outside surface of the shell.

Initially perfect shells may buckle at pressures approaching 43 percent greater than the pressure given by this empirical equation. However, it appears unrealistic to rely on this additional strength because of the difficulty in measuring the initial contours of most practical shells to the degree of accuracy required.

Based on the results of the elastic buckle specimens, an empirical formula was also developed which adequately predicted the collapse of near-perfect machined hemispherical shells which had ideal boundaries and which failed at stress levels above the proportional limit. This formula may be expressed as

$$P_E = 0.84 \sqrt{E_s E_t} \quad (h/R_o)^2 \quad \text{for } \nu = 0.3 \qquad [A\ 3]$$

For stress levels below the proportional limit, Equation [A 3] reduces to Equation [A 2]. From simple equilibrium, the average stress may be expressed as

$$\sigma_{avg} = \frac{p\, R_o^2}{2h\, R} \qquad [A\ 4]$$

Equation [A 3] can then be solved by a trial and error process using the stress-strain curve for the material used in the test specimen. Equation [A 3] therefore provides a baseline for predicting the elastic or inelastic collapse of near-perfect, initially stress-free, deep spherical shells with ideal boundaries.

Tests were also conducted to determine the relationship between unsupported arc length and the elastic and inelastic collapse strength of machined shallow spherical caps with clamped edges.[1,5] Although previous data in the literature showed wide disagreement in experimental results, these tests followed a very definite pattern. The test results for the elastic models are plotted in Figure A-1.[5] The ordinate is the ratio of the experimental collapse pressure to the empirical pressure P_3, and the abscissa is the nondimensional parameter θ defined as

$$\theta = \frac{0.91\ L_a}{\sqrt{Rh}} \quad \text{for} \quad \nu = 0.3 \qquad [A\ 5]$$

where L_a is the unsupported arc length of the shell. The results are in good agreement with the axisymmetric nonlinear theory of Budiansky,[6] Weinitschke,[7] and Thurston[8] for θ less than about 5.5 and the nonsymmetric nonlinear theory of Huang[9] and Thurston[10] for θ greater than 5.5. Thus, it seems reasonable to assume that the mode of failure becomes nonsymmetric for θ greater than 5.5. The experimental results for the inelastic models are presented in Figure 7.[1] The results are plotted in families of curves which basically represent varying degrees of stability; shells with the highest values of P_3/P_E are the most stable. For those deep segments which had P_3/P_E ratios of 1, the average membrane stress at collapse was approximately 70 percent of the proportional limit. The observed collapse pressure was approximately 20 percent lower than would be expected for a complete near-perfect sphere.

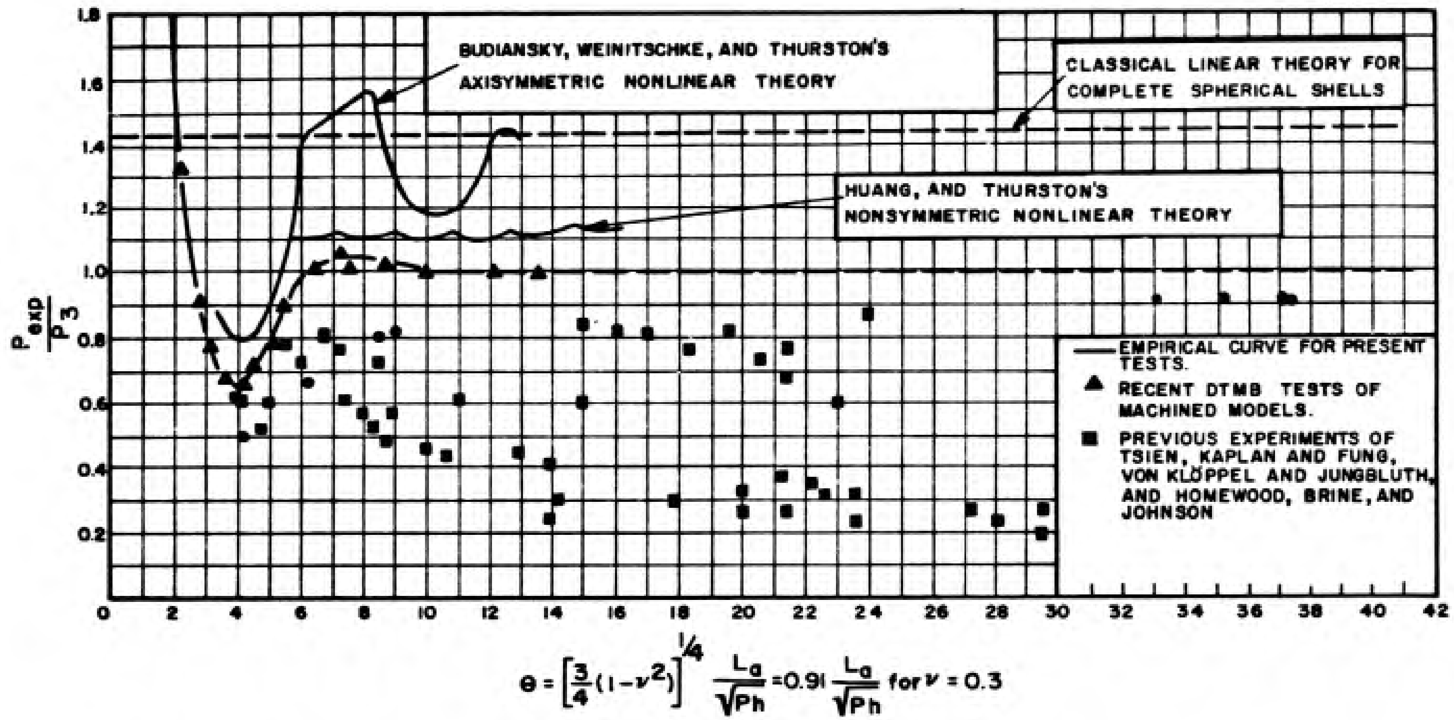

Figure A-1 – Experimental Elastic Buckling Data for Spherical Shells with Clamped Edges

APPENDIX B
STRESS ANALYSIS OF SPHERICAL SEGMENTS

The forces and moments in a spherical segment with clamped edges under external hydrostatic loading can be obtained by superimposing the results of the membrane and bending solutions such that the boundary conditions are satisfied. In the membrane problem (Figure B-1) the shell experiences a uniform compression, no rotation at the edge, and a horizontal displacement given by

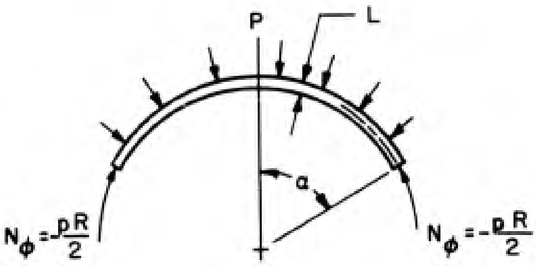

FIGURE B-1

$$\delta = -\frac{pR^2(1-\nu)}{2Eh}\sin\alpha \qquad [B\ 1]$$

To this solution must now be added the effects of edge moment and horizontal force consistent with the boundary conditions (Figure B-2).

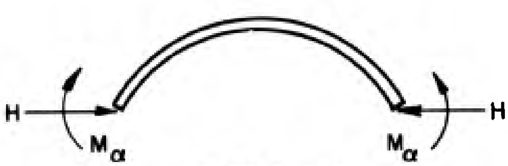

FIGURE B-2

The magnitude of H and M_α must be such that the corresponding rotation and horizontal displacement at the edge are zero.

The analysis of a spherical shell under symmetrical loading is presented by Timoshenko in Reference 11. Of interest to this report is an approximate solution obtained by Hetenyi.[12] The results of his solution for the forces, moments, horizontal displacement, and rotation are:

$$N_\phi = -\cot(\alpha - \psi)\, C \frac{e^{-\lambda\psi}}{\sqrt{\sin(\alpha - \psi)}} \sin(\lambda\psi + \gamma) \qquad [B\ 2]$$

$$N_\theta = C \frac{\lambda e^{-\lambda\psi}}{2\sqrt{\sin(\alpha - \psi)}} \left[2\cos(\lambda\psi + \gamma) - (K_1 + K_2)\sin(\lambda\psi + \gamma)\right] \qquad [B\ 3]$$

$$M_\phi = \frac{R}{2\lambda} C \frac{e^{-\lambda\psi}}{\sqrt{\sin(\alpha - \psi)}} \left[K_1 \cos(\lambda\psi + \gamma) + \sin(\lambda\psi + \gamma)\right] \qquad [B\ 4]$$

$$M_\theta = \frac{R}{4\nu\lambda} C \frac{e^{-\lambda\psi}}{\sqrt{\sin(\alpha - \psi)}} \Big\{\left[(1 + \nu^2)(K_1 + K_2) - 2K_2\right]\cos(\lambda\psi + \gamma)$$

$$+ 2\nu^2 \sin(\lambda\psi + \gamma)\Big\} \qquad [B\ 5]$$

$$\delta = \frac{R\sin(\alpha - \psi)}{Eh} C \frac{\lambda e^{-\lambda\psi}}{\sqrt{\sin(\alpha - \psi)}} \left[\cos(\lambda\psi + \gamma) - K_2 \sin(\lambda\psi + \gamma)\right] \qquad [B\ 6]$$

$$V = -\frac{2\lambda^2}{Eh} C \frac{e^{-\lambda\psi}}{\sqrt{\sin(\alpha - \psi)}} \cos(\lambda\psi + \gamma) \qquad [B\ 7]$$

where the angles α, ϕ, and ψ are defined as shown,

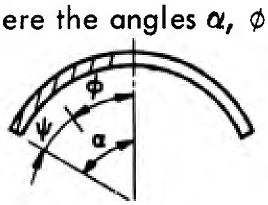

and

$$K_1 = 1 - \frac{1 - 2\nu}{2\lambda} \cot(\alpha - \psi) \qquad [B\ 8]$$

$$K_2 = 1 - \frac{1 + 2\nu}{2\lambda} \cot(\alpha - \psi) \qquad [B\ 9]$$

$$\lambda^4 = 3(1 - \nu^2)\left(\frac{R}{h}\right)^2 \qquad [B\ 10]$$

The constants C and γ are determined from edge conditions. For the case of horizontal force applied to the edge of the shell, the boundary conditions are:

$$(M_\phi)_{\phi = \alpha} = 0 \qquad\qquad (N_\phi)_{\phi = \alpha} = -H \cos\alpha$$

Substitution of the first condition into Equation [B 4] gives γ. γ and the second condition can then be substituted into Equation [B 2] to determine C. These operations give

$$\gamma_H = \tan^{-1} K_1 \qquad [B\ 11]$$

$$C_H = -H(\sin\alpha)^{\frac{3}{2}} \frac{\sqrt{K_1^2 + 1}}{K_1} \qquad [B\ 12]$$

The horizontal displacement and rotation at the edge are then found to be:

$$\delta_H = -\frac{\lambda R \sin^2\alpha}{Eh}\left(K_2 + \frac{1}{K_1}\right) H \qquad [B\ 13]$$

$$V_H = \frac{2\lambda^2 \sin\alpha}{Eh K_1} H \qquad [B\ 14]$$

For the case of moments distributed along the edge, the boundary conditions are:

$$(M_\phi)_{\phi = \alpha} = M_\alpha \qquad\qquad (N_\phi)_{\phi = \alpha} = 0$$

Proceeding in a manner similar to that described above, the constants for this case are given by:

$$\gamma_m = 0 \qquad [B\ 15]$$

$$C_m = \frac{2\lambda M_\alpha \sqrt{\sin\alpha}}{R\, K_1} \qquad [B\ 16]$$

The horizontal displacement and rotation at the edge follow:

$$\delta_m = \frac{2\lambda^2 \sin\alpha}{Eh\, K_1} M_\alpha \qquad [B\ 17]$$

$$V_m = \frac{-4\lambda^3 M_\alpha}{ERh\, K_1} \qquad [B\ 18]$$

The edge moment M_α and the horizontal force H can now be determined from the boundary conditions for a clamped spherical segment. These require zero horizontal displacement and rotation at the edge.

$$\Sigma\delta = 0: \quad \frac{-\lambda R \sin^2\alpha}{Eh}\left(K_2 + \frac{1}{K_1}\right) H + \frac{2\lambda^2 \sin\alpha}{Eh\, K_1} M_\alpha = \frac{pR^2(1-\nu)}{2Eh} \sin\alpha \qquad [B\ 19]$$

$$\Sigma V = 0: \quad \frac{2\lambda^2 \sin\alpha}{Eh\, K_1} H - \frac{4\lambda^3 M_\alpha}{ERh\, K_1} = 0 \qquad [B\ 20]$$

These equations give

$$M_\alpha = \frac{-pR^2 (1 - \nu)}{4\lambda^2 K_2} \qquad [B\ 21]$$

$$H = \frac{-pR (1 - \nu)}{2\lambda K_2 \sin \alpha} \qquad [B\ 22]$$

In the two sets of constants of γ and C, C_H and C_m may now be evaluated from these relations. Superposition of the forces and moments found from each set with the results of the membrane theory yield the forces and moments for the spherical segment with clamped boundaries under hydrostatic loading. The results are:

$$N_\phi = -\frac{pR}{2} + \frac{e^{-\lambda\psi} pR (1 - \nu)}{2\lambda} \cot (\alpha - \psi) \left[\frac{\sqrt{\sin \alpha}}{K_2 \sqrt{\sin (\alpha - \psi)}} \right] \cos \lambda\psi \qquad [B\ 23]$$

$$N_\theta = -\frac{pR}{2} + \frac{e^{-\lambda\psi} pR (1 - \nu)\sqrt{\sin \alpha}}{4K_2 \sqrt{\sin (\alpha - \psi)}} [\, 2 \sin \lambda\psi + (K_1 + K_2) \cos \lambda\psi \,] \qquad [B\ 24]$$

$$M_\phi = \frac{e^{-\lambda\psi} pR^2 (1 - \nu) \sqrt{\sin \alpha}}{4\lambda^2 K_2 \sqrt{\sin (\alpha - \psi)}} (K_1 \sin \lambda\psi - \cos \lambda\psi) \qquad [B\ 25]$$

$$M_\theta = \frac{e^{-\lambda\psi} pR^2 (1 - \nu) \sqrt{\sin \alpha}}{8 \nu \lambda^2 K_2 \sqrt{\sin (\alpha - \psi)}} \left\{ \left[(1 + \nu^2) (K_1 + K_2) - 2K_2 \right] \sin \lambda\psi - 2\nu^2 \cos \lambda\psi \right\} \qquad [B\ 26]$$

The strains can readily be obtained from these equations and the two-dimensional Hooke's Law. Equations [B 23] - [B 26] were programmed for the high-speed computer facilities of the Applied Mathematics Laboratory at the Model Basin. It is apparent that these equations do not yield valid answers for certain angles. When the right term of the right side of Equation [B 9] becomes 1, K_2, which appears as a denominator for each of these equations, becomes zero and yields infinite values for the forces and moments. Also, when the angle $(\alpha - \psi)$ becomes zero (at the apex), the term $\sqrt{\sin (\alpha - \psi)}$ becomes zero, again yielding infinite values for the forces and moments. For the two geometries studied, K_2 becomes zero at approximately 5 deg from the apex. The results obtained from these equations in these areas have been ignored in the curves of Figure 4 since membrane conditions were prevalent. The curves were completed by arbitrarily assuming the membrane strain.

REFERENCES

1. Krenzke, M.A. and Kiernan, T.J., "Tests of Stiffened and Unstiffened Machined Spherical Shells under External Hydrostatic Pressure," David Taylor Model Basin Report 1741 (Aug 1963).

2. Timoshenko, S., "Theory of Elastic Stability," McGraw-Hill Book Company, Inc., New York (1936).

3. Krenzke, M.A., "Tests of Machined Deep Spherical Shells under External Hydrostatic Pressure," David Taylor Model Basin Report 1601 (May 1962).

4. Krenzke, M.A., "The Elastic Buckling Strength of Near-Perfect Deep Spherical Shells with Ideal Boundaries," David Taylor Model Basin Report 1713 (Jul 1963).

5. Krenzke, M.A. and Kiernan, T.J., "Elastic Stability of Near-Perfect Shallow Spherical Shells," American Institute of Aeronautics and Astronautics Journal, Vol. 1, No. 12, p. 2857 (Dec 1963).

6. Budiansky, B., "Buckling of Clamped Shallow Spherical Shells," Proceedings of the IUTAM Symposium of the Theory of Thin Elastic Shells (North Holland Publishing Co., Amsterdam, 1960) p. 64.

7. Weinitschke, H., "On the Stability Problem for Shallow Spherical Shells," J. Math. Phys. 38, 209 (Jan 1960).

8. Thurston, G.A., "A Numerical Solution of the Nonlinear Equations for Axisymmetric Bending of Shallow Spherical Shells," J. Appl. Mech. 28, 557 (Dec 1961).

9. Huang, N.C., "Unsymmetrical Buckling of Thin Shallow Spherical Shells," Tech Report 15, Harvard Univ. (Mar 1963).

10. Thurston, G.A., "Asymmetrical Buckling of Spherical Caps under Uniform Pressure," American Institute of Aeronautics and Astronautics Journal, Vol. 2, No. 10, p. 1832 (Oct 1964).

11. Timoshenko, S., "Theory of Plates and Shells," McGraw-Hill Book Company, Inc., New York (1959).

12. Hetenyi, M., "Publs. Intern. Assoc. Bridge Structural Engrs.," Vol. 5, p. 173 (1938).

INITIAL DISTRIBUTION

Copies

15 CHBUSHIPS
- 2 Sci & Res (Code 442)
- 1 Lab Mgt (Code 320)
- 3 Tech Lib (Code 210L)
- 1 Struc Mech, Hull Mat & Fab (Code 341A)
- 1 Prelim Des Br (Code 420)
- 1 Prelim Des Sec (Code 421)
- 1 Ship Protec (Code 423)
- 1 Hull Des Br (Code 440)
- 1 Struc Sec (Code 443)
- 2 Sub Br (Code 525)
- 1 Pres Ves Sec (Code 651F)

2 CHONR
- 1 Struc Mech Br (Code 439)
- 1 Undersea Programs (Code 466)

4 CNO
- 1 Plans, Programs & Req Br (Op 311)
- 1 Tech Anal & Adv Gr (Op 07T)
- 1 Sub Program Br (Op 713)
- 1 Tech Support Br (Op 725)

20 CDR, DDC

1 CO & DIR, USNMEL

1 CDR, USNOL

1 DIR, USNRL (Code 2027)

1 CO & DIR, USNUSL

1 CO & DIR, USNEL

1 CDR, USNOTS, China Lake

1 CDR, USNOTS, Pasadena

1 CO, USNUOS

2 NAVSHIPYD PTSMH

2 NAVSHIPYD MARE

1 NAVSHIPYD CHASN

1 SUPSHIP, Groton

1 EB Div, Gen Dyn Corp

1 SUPSHIP, Newport News

1 NNSB & DD Co

Copies

1 SUPSHIP, Pascagoula

1 Ingalls Shipbldg Corp

1 SUPSHIP, Camden

1 New York Shipbldg

1 DIR DEF, R&E, Attn: Tech Library

1 CO, USNROTC & NAVADMINU, MIT

1 O in C, PGSCOL, Webb

1 DIR, APL, Univ of Washington, Seattle

1 NAS, Attn: Comm on Undersea Warfare

1 Prof. J. Kempner, Polytechnic Institute of Brooklyn

1 Dr. R. DeHart, SWRI

1 Mr. Leonard P. Zick, Chicago Bridge & Iron Co.

1 Dean V.L. Salerno, Fairleigh Dickinson Univ.

1 Prof. E.O. Waters, Yale Univ.

2 Mr. C.F. Larson, Sec, Welding Res Council

1 Prof. Bernard Budiansky, Harvard Univ.

1 Mr. J. Mavor, WHOI

UNCLASSIFIED

Security Classification

DOCUMENT CONTROL DATA - R&D

(Security classification of title, body of abstract and indexing annotation must be entered when the overall report is classified)

1. ORIGINATING ACTIVITY *(Corporate author)* Department of the Navy David Taylor Model Basin Washington, D.C.	2a. REPORT SECURITY CLASSIFICATION Unclassified 2b. GROUP

3. REPORT TITLE

TESTS OF MACHINED MULTILAYER SPHERICAL SHELLS WITH CLAMPED BOUNDARIES UNDER EXTERNAL HYDROSTATIC PRESSURE

4. DESCRIPTIVE NOTES *(Type of report and inclusive dates)*

Final

5. AUTHOR(S) *(Last name, first name, initial)*

Nishida, Kanehiro

6. REPORT DATE	7a. TOTAL NO. OF PAGES	7b. NO. OF REFS
August 1965	41	11

8a. CONTRACT OR GRANT NO. S-R011 01 01 b. PROJECT NO. 1-725-238-01 c. Task 0401 d.	9a. ORIGINATOR'S REPORT NUMBER(S) 2012 9b. OTHER REPORT NO(S) *(Any other numbers that may be assigned this report)* None

10. AVAILABILITY/LIMITATION NOTICES

No Limitations

11. SUPPLEMENTARY NOTES	12. SPONSORING MILITARY ACTIVITY David Taylor Model Basin Director's Research

13. ABSTRACT

Six spherical shell models with clamped boundaries consisting of two and four layers were tested under external hydrostatic pressure to explore the feasibility of multilayer construction for application to hydrospace vehicles. In addition, four monolithic models were tested to provide a basis of comparison. Three of the multilayer shells were bonded with epoxy resin and the remaining three were not bonded. The bonded multilayer shell models collapsed at pressures ap, roximately equal to that of the monolithic shells. The unbonded shells showed appreciable reduction in strength.

DD FORM 1 JAN 64 1473

UNCLASSIFIED

Security Classification

14. KEY WORDS	LINK A		LINK B		LINK C	
	ROLE	WT	ROLE	WT	ROLE	WT
Multilayer Spherical Shells						
Elastic Buckling of Spherical Shells						
Inelastic Buckling of Spherical Shells						
Collapse of Spherical Shells						
Collapse of Multilayer Spherical Segments						

INSTRUCTIONS

1. ORIGINATING ACTIVITY: Enter the name and address of the contractor, subcontractor, grantee, Department of Defense activity or other organization *(corporate author)* issuing the report.

2*a*. REPORT SECURITY CLASSIFICATION: Enter the overall security classification of the report. Indicate whether "Restricted Data" is included. Marking is to be in accordance with appropriate security regulations.

2*b*. GROUP: Automatic downgrading is specified in DoD Directive 5200.10 and Armed Forces Industrial Manual. Enter the group number. Also, when applicable, show that optional markings have been used for Group 3 and Group 4 as authorized.

3. REPORT TITLE: Enter the complete report title in all capital letters. Titles in all cases should be unclassified. If a meaningful title cannot be selected without classification, show title classification in all capitals in parenthesis immediately following the title.

4. DESCRIPTIVE NOTES: If appropriate, enter the type of report, e.g., interim, progress, summary, annual, or final. Give the inclusive dates when a specific reporting period is covered.

5. AUTHOR(S): Enter the name(s) of author(s) as shown on or in the report. Enter last name, first name, middle initial. If military, show rank and branch of service. The name of the principal author is an absolute minimum requirement.

6. REPORT DATE: Enter the date of the report as day, month, year; or month, year. If more than one date appears on the report, use date of publication.

7*a*. TOTAL NUMBER OF PAGES: The total page count should follow normal pagination procedures, i.e., enter the number of pages containing information.

7*b*. NUMBER OF REFERENCES: Enter the total number of references cited in the report.

8*a*. CONTRACT OR GRANT NUMBER: If appropriate, enter the applicable number of the contract or grant under which the report was written.

8*b*, 8*c*, & 8*d*. PROJECT NUMBER: Enter the appropriate military department identification, such as project number, subproject number, system numbers, task number, etc.

9*a*. ORIGINATOR'S REPORT NUMBER(S): Enter the official report number by which the document will be identified and controlled by the originating activity. This number must be unique to this report.

9*b*. OTHER REPORT NUMBER(S): If the report has been assigned any other report numbers *(either by the originator or by the sponsor)*, also enter this number(s).

10. AVAILABILITY/LIMITATION NOTICES: Enter any limitations on further dissemination of the report, other than those imposed by security classification, using standard statements such as:

(1) "Qualified requesters may obtain copies of this report from DDC."

(2) "Foreign announcement and dissemination of this report by DDC is not authorized."

(3) "U. S. Government agencies may obtain copies of this report directly from DDC. Other qualified DDC users shall request through
_______________________________."

(4) "U. S. military agencies may obtain copies of this report directly from DDC. Other qualified users shall request through
_______________________________."

(5) "All distribution of this report is controlled. Qualified DDC users shall request through
_______________________________."

If the report has been furnished to the Office of Technical Services, Department of Commerce, for sale to the public, indicate this fact and enter the price, if known.

11. SUPPLEMENTARY NOTES: Use for additional explanatory notes.

12. SPONSORING MILITARY ACTIVITY: Enter the name of the departmental project office or laboratory sponsoring *(paying for)* the research and development. Include address.

13. ABSTRACT: Enter an abstract giving a brief and factual summary of the document indicative of the report, even though it may also appear elsewhere in the body of the technical report. If additional space is required, a continuation sheet shall be attached.

It is highly desirable that the abstract of classified reports be unclassified. Each paragraph of the abstract shall end with an indication of the military security classification of the information in the paragraph, represented as *(TS)*, *(S)*, *(C)*, or *(U)*.

There is no limitation on the length of the abstract. However, the suggested length is from 150 to 225 words.

14. KEY WORDS: Key words are technically meaningful terms or short phrases that characterize a report and may be used as index entries for cataloging the report. Key words must be selected so that no security classification is required. Identifiers, such as equipment model designation, trade name, military project code name, geographic location, may be used as key words but will be followed by an indication of technical context. The assignment of links, roles, and weights is optional.

David Taylor Model Basin. Report 2012.
TESTS OF MACHINED MULTILAYER SPHERICAL SHELLS WITH CLAMPED BOUNDARIES UNDER EXTERNAL HYDROSTATIC PRESSURE, by Kanehiro Nishida. Aug 1965. iii, 41p. illus., diagrs., graphs, refs. UNCLASSIFIED

Six spherical shell models with clamped boundaries consisting of two and four layers were tested under external hydrostatic pressure to explore the feasibility of multilayer construction for application to hydrospace vehicles. In addition, four monolithic models were tested to provide a basis of comparison. Three of the multilayer shells were bonded with epoxy resin and the remaining three were not bonded. The bonded multilayer shell models collapsed at pressures approximately equal to that of the monolithic shells. The unbonded shells showed appreciable reduction in strength.

1. Spherical shells (Laminated)--Buckling--Model tests
2. Spherical shells (Laminated)--Collapse--Model tests
3. Spherical shells (Laminated)--Hydrostatic pressure--Model tests
4. Hydrospace vehicles
I. Nishida, Kanehiro
II. S-R011 01 01

David Taylor Model Basin. Report 2012.
TESTS OF MACHINED MULTILAYER SPHERICAL SHELLS WITH CLAMPED BOUNDARIES UNDER EXTERNAL HYDROSTATIC PRESSURE, by Kanehiro Nishida. Aug 1965. iii, 41p. illus., diagrs., graphs, refs. UNCLASSIFIED

Six spherical shell models with clamped boundaries consisting of two and four layers were tested under external hydrostatic pressure to explore the feasibility of multilayer construction for application to hydrospace vehicles. In addition, four monolithic models were tested to provide a basis of comparison. Three of the multilayer shells were bonded with epoxy resin and the remaining three were not bonded. The bonded multilayer shell models collapsed at pressures approximately equal to that of the monolithic shells. The unbonded shells showed appreciable reduction in strength.

1. Spherical shells (Laminated)--Buckling--Model tests
2. Spherical shells (Laminated)--Collapse--Model tests
3. Spherical shells (Laminated)--Hydrostatic pressure--Model tests
4. Hydrospace vehicles
I. Nishida, Kanehiro
II. S-R011 01 01

David Taylor Model Basin. Report 2012.
TESTS OF MACHINED MULTILAYER SPHERICAL SHELLS WITH CLAMPED BOUNDARIES UNDER EXTERNAL HYDROSTATIC PRESSURE, by Kanehiro Nishida. Aug 1965. iii, 41p. illus., diagrs., graphs, refs. UNCLASSIFIED

Six spherical shell models with clamped boundaries consisting of two and four layers were tested under external hydrostatic pressure to explore the feasibility of multilayer construction for application to hydrospace vehicles. In addition, four monolithic models were tested to provide a basis of comparison. Three of the multilayer shells were bonded with epoxy resin and the remaining three were not bonded. The bonded multilayer shell models collapsed at pressures approximately equal to that of the monolithic shells. The unbonded shells showed appreciable reduction in strength.

1. Spherical shells (Laminated)--Buckling--Model tests
2. Spherical shells (Laminated)--Collapse--Model tests
3. Spherical shells (Laminated)--Hydrostatic pressure--Model tests
4. Hydrospace vehicles
I. Nishida, Kanehiro
II. S-R011 01 01

David Taylor Model Basin. Report 2012.
TESTS OF MACHINED MULTILAYER SPHERICAL SHELLS WITH CLAMPED BOUNDARIES UNDER EXTERNAL HYDROSTATIC PRESSURE, by Kanehiro Nishida. Aug 1965. iii, 41p. illus., diagrs., graphs, refs. UNCLASSIFIED

Six spherical shell models with clamped boundaries consisting of two and four layers were tested under external hydrostatic pressure to explore the feasibility of multilayer construction for application to hydrospace vehicles. In addition, four monolithic models were tested to provide a basis of comparison. Three of the multilayer shells were bonded with epoxy resin and the remaining three were not bonded. The bonded multilayer shell models collapsed at pressures approximately equal to that of the monolithic shells. The unbonded shells showed appreciable reduction in strength.

1. Spherical shells (Laminated)--Buckling--Model tests
2. Spherical shells (Laminated)--Collapse--Model tests
3. Spherical shells (Laminated)--Hydrostatic pressure--Model tests
4. Hydrospace vehicles
I. Nishida, Kanehiro
II. S-R011 01 01